

Adaptive Noise Reduction Techniques for Airborne Acoustic Sensors

A thesis submitted in partial fulfillment
of the requirements for the degree of
Master of Science in Engineering

by

Ryan M. Fuller

B.S. Applied Mathematics, Rochester Institute of Technology, 2006

2012
Wright State University

Report Documentation Page				Form Approved OMB No. 0704-0188	
Public reporting burden for the collection of information is estimated to average 1 hour per response, including the time for reviewing instructions, searching existing data sources, gathering and maintaining the data needed, and completing and reviewing the collection of information. Send comments regarding this burden estimate or any other aspect of this collection of information, including suggestions for reducing this burden, to Washington Headquarters Services, Directorate for Information Operations and Reports, 1215 Jefferson Davis Highway, Suite 1204, Arlington VA 22202-4302. Respondents should be aware that notwithstanding any other provision of law, no person shall be subject to a penalty for failing to comply with a collection of information if it does not display a currently valid OMB control number.					
1. REPORT DATE 2012		2. REPORT TYPE		3. DATES COVERED 00-00-2012 to 00-00-2012	
4. TITLE AND SUBTITLE Adaptive Noise Reduction Techniques for Airborne Acoustic Sensor				5a. CONTRACT NUMBER	
				5b. GRANT NUMBER	
				5c. PROGRAM ELEMENT NUMBER	
6. AUTHOR(S)				5d. PROJECT NUMBER	
				5e. TASK NUMBER	
				5f. WORK UNIT NUMBER	
7. PERFORMING ORGANIZATION NAME(S) AND ADDRESS(ES) Wright State University, Department of Electrical Engineering, Dayton, OH, 45435				8. PERFORMING ORGANIZATION REPORT NUMBER	
9. SPONSORING/MONITORING AGENCY NAME(S) AND ADDRESS(ES)				10. SPONSOR/MONITOR'S ACRONYM(S)	
				11. SPONSOR/MONITOR'S REPORT NUMBER(S)	
12. DISTRIBUTION/AVAILABILITY STATEMENT Approved for public release; distribution unlimited					
13. SUPPLEMENTARY NOTES					
14. ABSTRACT Ground and marine based acoustic arrays are currently employed in a variety of military and civilian applications for the purpose of locating and identifying sources of interest. An airborne acoustic array could perform an identical role, while providing the ability to cover a larger area and pursue a target. In order to implement such a system, steps must be taken to attenuate environmental noise that interferes with the signal of interest. In this thesis, we discuss the noise sources present in an airborne environment, present currently available methods for mitigation of these sources, and propose the use of adaptive noise cancellation techniques for removal of unwanted wind and engine noise. The least mean squares, affine projection, and extended recursive least squares algorithms are tested on recordings made aboard an airplane in-flight, and the results are presented. The algorithms provide upwards of 37dB of noise cancellation, and are able to filter the noise from a chirp with a signal to noise ratio of -20db with minimal mean square error. The experiment demonstrates that adaptive noise cancellation techniques are an effective method of suppressing unwanted acoustic noise in an airborne environment, but due to the complexity of the environment more sophisticated algorithms may be warranted. iii					
15. SUBJECT TERMS					
16. SECURITY CLASSIFICATION OF:			17. LIMITATION OF ABSTRACT Same as Report (SAR)	18. NUMBER OF PAGES 80	19a. NAME OF RESPONSIBLE PERSON
a. REPORT unclassified	b. ABSTRACT unclassified	c. THIS PAGE unclassified			

Wright State University
GRADUATE SCHOOL

August 7, 2012

I HEREBY RECOMMEND THAT THE THESIS PREPARED UNDER MY SUPERVISION BY Ryan M. Fuller ENTITLED Adaptive Noise Reduction Techniques for Airborne Acoustic Sensors BE ACCEPTED IN PARTIAL FULFILLMENT OF THE REQUIREMENTS FOR THE DEGREE OF Master of Science in Engineering.

Brian D. Rigling, Ph.D.
Thesis Director

Kefu Xue, Ph.D.
Department Chair of Electrical Engineering

Committee on
Final Examination

Brian D. Rigling , Ph.D.

Kefu Xue , Ph.D.

Fred Garber , Ph.D.

Andrew T. Hsu, Ph.D.
Dean, Graduate School

ABSTRACT

Fuller, Ryan M. , M.S.Egr, Department of Electrical Engineering, Wright State University, 2012 . *Adaptive Noise Reduction Techniques for Airborne Acoustic Sensors*.

Ground and marine based acoustic arrays are currently employed in a variety of military and civilian applications for the purpose of locating and identifying sources of interest. An airborne acoustic array could perform an identical role, while providing the ability to cover a larger area and pursue a target. In order to implement such a system, steps must be taken to attenuate environmental noise that interferes with the signal of interest. In this thesis, we discuss the noise sources present in an airborne environment, present currently available methods for mitigation of these sources, and propose the use of adaptive noise cancellation techniques for removal of unwanted wind and engine noise. The least mean squares, affine projection, and extended recursive least squares algorithms are tested on recordings made aboard an airplane in-flight, and the results are presented. The algorithms provide upwards of 37dB of noise cancellation, and are able to filter the noise from a chirp with a signal to noise ratio of -20db with minimal mean square error. The experiment demonstrates that adaptive noise cancellation techniques are an effective method of suppressing unwanted acoustic noise in an airborne environment, but due to the complexity of the environment more sophisticated algorithms may be warranted.

Contents

1	Introduction	1
1.1	Contribution	2
1.2	Outline	3
2	Previous Work	5
2.1	Passive Means of Attenuating Environmental Interference	5
2.2	Active Methods for Attenuation of Environmental Interference	6
2.2.1	Spatial Filtering	6
2.2.2	Adaptive Noise Cancellation for Signal Enhancement	7
2.3	Currently Available Systems	8
2.3.1	Helicopter Alert and Threat Termination (HALTT)	8
2.3.2	Boomerang	8
2.3.3	Low Cost Scout UAV Acoustics System (LOSAS)	8
2.3.4	Shot Spotter	9
2.3.5	Shot Stalker	9
3	Acoustic Fundamentals and Recording	10
3.1	Sound Propagation Through Atmosphere	10
3.2	Classification of Sound Sources	13
3.3	Audio Recording	15
3.3.1	Audio Microphones and Preamplifiers	16
3.3.2	Audio Recorders	20

4	Noise in an Airborne Environment	22
4.1	Environmental Noise Interference	22
4.1.1	Wind Noise	23
4.1.2	Aircraft Noise	24
4.2	Airborne Test Platforms	25
4.2.1	Super Cub Test Platform	25
4.2.2	Monocoupe Test Platform	26
5	Adaptive Noise Cancellation	31
5.1	Fundamentals of Adaptive Noise Cancellation	31
5.2	Adaptive Algorithms	33
5.2.1	Least Mean Squares Algorithm	36
5.2.2	Affine Projection Algorithm	37
5.2.3	Extended Recursive Least Squares Type-1 Algorithm	38
6	Experimental Validation of Effectiveness of Adaptive Algorithms	40
6.1	Preliminary Experiments	40
6.2	Flight Test Setup	41
6.3	Flight Test	46
6.4	Analysis	48
6.4.1	Noise Cancellation	48
6.4.2	Signal Enhancement for Additive Chirp	50
7	Conclusion	56
A	Matlab Code for Adaptive Algorithms	58
A.1	Normalized Least Mean Squares Program	58
A.2	Affine Projection Program	60
A.3	Extended Recursive Least Squares Type-1 Program	62
	Bibliography	65

List of Figures

3.1	Illustration of inverse square law relation of sound intensity to distance.	11
3.2	Attenuation of sound in air increases with frequency (figure from [1]).	12
3.3	Attenuation of 250Hz sound in air decreases with increasing temperature (figure from [1]).	12
3.4	Attenuation of 1kHz sound in air decreases with increasing humidity (figure from [1]).	13
3.5	Audible frequency range and hearing range of various sources (figure from [2]). . .	14
3.6	Approximate intensity of various sound sources (figure from [2]).	14
3.7	Sound pressure level of conversation, with a reference SPL of 65dB at 1 meter, as a function of distance.	15
3.8	Directionality of microphone types: (a) omnidirectional; (b) subcardioid; (c) cardioid; (d) supercardioid; (e) bidirectional; (f) shotgun.	17
3.9	Frequency response of Audio Technica Pro 42 boundary microphone (figure from [3]).	17
4.1	Comparison of turbulent and laminar fluid flow.	23
4.2	Super Cub LP RTF RC Airplane [4]	25
4.3	Super Kraft Monocoupe 90A RC airplane.	27
4.4	Access panel for fuselage of Monocoupe 90A.	27
4.5	Sound spectrum of monocoupe in-flight (Relative Intensity (dB) vs. Frequency (Hz)).	29
4.6	Spectrogram of Monocoupe in-flight using a Hanning window of length 4096 (Frequency (kHz) vs. Time (s)).	29

4.7	Spectral bands produced by Monocoupe engine using a Hanning window of length 16384 (Frequency (Hz) vs. Time (s)).	30
5.1	Block diagram of generic adaptive noise cancellation concept.	32
5.2	Block diagram of generic adaptive filter.	33
6.1	Recording device setup.	43
6.2	Placement of the microphones within Monocoupe chassis.	44
6.3	Placement of the recorder and GPS within Monocoupe chassis.	44
6.4	Recorded flight path for experiment with second of latitude/longitude lines in pink	47
6.5	Recorded altitude (above sea level) and velocity during experiment.	48
6.6	Spectrogram of reference signal of low-speed recording with 9-second chirp and SNR=-20dB using a Hanning window of length 4096 (Frequency [kHz] vs. Time [s]).	52
6.7	Spectrogram (using Hanning window of length 4096) of cruise speed recording with -20dB chirp, filtered with LMS (Frequency [kHz] vs Time [s]).	54
6.8	Spectrum of cruise speed recording with -20dB chirp, filtered with LMS.	54
6.9	Spectrum of cruise speed recording with -20dB chirp, filtered with APA.	55
6.10	Spectrum of cruise speed recording with -20dB chirp, filtered with ERLS-1.	55

Acknowledgement

Air Force Research Laboratory - Air Vehicles Directorate

Raymond Bortner

Bryan Cannon

Air Force Research Laboratory - Propulsion Directorate

Keith Numbers

Air Force Research Laboratory - 711th Human Performance Wing

Frank Mobley

Ken Johnson

Dedicated to
James and Amy Fuller
and
Jillian Marconi

Chapter 1

Introduction

One of the traditional applications for UAVs is to serve as platforms for remote sensing and surveillance. For this purpose, a broad range of sensors are available that provide radio frequency, optical, infrared, chemical, biological, and nuclear information. The data gathered by these sensors provide decision makers with greater situational awareness of the theatre in which they are employed.

Notably absent from the list of available sensors for UAVs is an acoustic array. An airborne acoustic sensor package could provide valuable signal intelligence to the UAV operator, and could be used to identify vehicles, detect gunshots, and eavesdrop upon conversations taking place on the ground. Additionally, an acoustic array could be used to identify and localize other aircraft for the purpose of collision avoidance, and since an acoustic array is a passive sensor, it could perform this tasks while consuming less energy than active systems such as radar, lidar, or sonar [5].

Ground and marine-based acoustic arrays are currently employed in a variety of military and civilian applications [6]. Airborne variants could be used for the same applications as ground-based systems, but there are additional benefits to fielding an acoustic system onboard an aerial platform. For example, such a system would be able to cover a much larger area than a ground-based system, and the UAV could be used to track the target over time. Also, sound is refracted upward during the day due to solar heating of the ground [7], so interference from obstacles such as buildings and foliage would be less of an issue. The benefits associated with an airborne acoustic sensor array are further discussed in [8].

The challenge in using microphones aboard a UAV is the noisy environment in which the aircraft operates. Engine, propellor, actuator, aeroacoustic, and wind noise all interfere with the signal of interest. Additionally, the distance to a target from which a UAV may be operating means that the sound source is significantly attenuated before reaching the aircraft. Factors affecting the performance of an airborne acoustic package can be classified into three groups: degradation of the signal of interest, additive noise inherent in the transduction and recording of audio, and interference with the signal. A list of factors that impede the performance of airborne acoustic sensors associated with each type is provided in Table 1.1.

Table 1.1: Impedance factors that affect performance of airborne acoustic sensors.

Type	Factor
Source Degradation	Distance Atmospheric Absorption
Recording Interference	Recorder Package Self Noise
Environmental Interference	Wind Noise Aerodynamics of Aircraft Engine Noise Propulsion Noise Actuation Noise Aircraft Vibration

From Table 1.1, the magnitude of the challenge of deploying acoustic microphones aboard UAVs for the purpose of remote sensing should be evident. Each of the problems associated with the source degradation and environmental interference factors must be addressed in order to develop an effective airborne acoustic sensor package. However, there are numerous active and passive techniques available for dealing with each of these interference sources, and many of them will be discussed in Chapter 2.

1.1 Contribution

The task of eavesdropping from an airborne platform is essentially one of signal enhancement. In this thesis, we study the various noise sources listed in Table 1.1 and document the methods that

currently exist for their mitigation. Due to the fact that all sources of environmental interference are indistinguishable to the microphone transducer [9], we propose that noise cancellation with adaptive algorithms could remove the unwanted environmental interference. The contribution of this work is to demonstrate the effectiveness of adaptive noise cancellation techniques at removing the combination of wind and aircraft noise for enhancement of a desired signal.

1.2 Outline

The remainder of this thesis discusses the factors affecting the implementation of an airborne acoustic array, and presents methods for mitigating the impedance factors presented in Table 1.1. Chapters 1 through 4 describe the problems inherent with using acoustic sensors on an airborne platform. The use of adaptive noise cancellation (ANC) techniques for attenuation of environmental noise is then proposed. Experimental validation of the effectiveness of the adaptive algorithms is performed, and the results are presented. It should be noted that the methods and information presented in this report are applicable to both fixed and rotary wing aircraft. A chapter by chapter outline of the thesis is as follows.

Chapter 2 - Previous Work

In this chapter, we discuss previous work and available methods for reduction of environmental noise interference. Additionally, we discuss currently available acoustic array systems and their performance and application.

Chapter 3 - Acoustic Fundamentals and Recording

The acoustic fundamentals necessary for this project are presented. Source degradation and recording interference are discussed as impedance factors, as well as methods for their attenuation. The limitations imposed by recording devices, as well as the nature of air as a medium, are presented in this chapter.

Chapter 4 - Noise in an Airborne Environment

Chapter 4 discusses the sources of environmental noise interference. The test platform for this project is presented, and the noise profile of the aircraft is examined.

Chapter 5 - Adaptive Noise Cancellation

The main contribution of this thesis—the proposed use of adaptive noise cancellation algorithms for environmental noise reduction—is presented in this chapter. The fundamentals of adaptive noise cancellation are discussed, and three algorithms are presented. Important considerations for implementation of adaptive noise cancellation are also considered.

Chapter 6 - Experimental Validation of Adaptive Algorithms

The test plan for the experiment used to validate the effectiveness of adaptive noise cancellation at attenuating environmental noise is presented. Recordings are made onboard an aircraft in flight, and the adaptive algorithms are tested on the collected data. An analysis of the effectiveness of the algorithms is presented in this chapter.

Chapter 7 - Conclusion

This report is concluded with a discussion of the experimental results. Additionally, a synopsis of the proposed methods of dealing with each source of noise interference is presented, and future work is discussed.

Chapter 2

Previous Work

Mitigation of unwanted noise is an area of concern for acoustic applications in environments with interference such as wind, engine, or other background noise. For this reason, a multitude of options exist for attenuation of unwanted noise. We will elaborate on both active and passive methods of noise reduction that are applicable to airborne acoustic sensing, and discuss their performance.

Although an acoustic array capable of airborne eavesdropping has yet to be successfully developed, a number of systems are currently in use which utilize microphones for the purposes discussed in Chapter 1. A description of the performance and intended application of these systems will provide a basis of comparison for the performance of an airborne acoustic array.

2.1 Passive Means of Attenuating Environmental Interference

Numerous devices and techniques are available that passively attenuate environmental noise from wind and generated by an aircraft. Devices such as windscreens and mufflers are intended to attenuate wind and engine noise, respectively. As discussion regarding the packaging of an airborne acoustic array and the aircraft propulsion method is beyond the scope of this thesis, we restrict ourselves to passive techniques for reducing the noise generated by the aerodynamics of the aircraft.

As most aircraft are not intended to be quiet, simple design changes can greatly reduce the amount of noise interference they generate.

Quieter Aircraft

Aeroacoustics is the study of noise generated by the turbulent flow of air. Aircraft noise is generally considered to be a nuisance, especially since many airports are located in urban areas, and for this reason a great deal of work has gone into studying aircraft aeroacoustics. The Silent Aircraft Initiative (silentaircraft.org) is an organization that is sponsored by the Cambridge-MIT Institute for the purpose of proposing a quieter aircraft design. Although the focus of this initiative is on large commercial aircraft, many of the proposed techniques are applicable to UAVs.

Resources on the airframe proposed by the Silent Aircraft Initiative can be found in [10]. Additionally, NASA has studied the problem and demonstrated 8dB of noise reduction using a combination of techniques in [11]. Additional resources can be found in [7].

2.2 Active Methods for Attenuation of Environmental Interference

Active methods of attenuating environmental noise include numerous signal processing techniques for noise suppression and enhancement of a desired signal. For the purpose of this project, we restrict ourselves to those methods that are intended for use in a non-stationary environment. The reason for this is discussed in [12]. These approaches include adaptive noise cancellation and beamforming. It should be noted that as of the writing of this thesis, no research has been found applying these techniques to airborne acoustic eavesdropping.

2.2.1 Spatial Filtering

Spatial filtering involves the augmentation or attenuation of sound depending on the angle of incidence, and one of the most effective signal processing techniques for spatial filtering is beamform-

ing. An excellent paper on the subject was written by Van Veen and Buckley [13], wherein they discuss data independent and statistically optimal beamforming. For a generic sensor array, Van Veen and Buckley demonstrate 30dB of directional gain using the data independent approach, as well as 70dB of attenuation of noise arriving from a known direction for the statistically optimal variant.

Beamforming with microphone arrays is an ongoing area of research in acoustics. Lustberg demonstrated directional gain of at least 20dB in the presence of pure sound tones by using a 29 microphone array [14], and Li and Chen simulated a beam-pattern with 20-40dB of directional gain using a frequency invariant approach and a 12 element array [15]. Kaneda and Ohga demonstrated 16dB of SNR improvement using the AMNOR approach and a 4-microphone array, for a speech signal corrupted by ambient white noise [16]. Additionally, Farrell simulated 11dB of SNR improvement for a speech signal that is corrupted by another speech source from a known direction [17].

2.2.2 Adaptive Noise Cancellation for Signal Enhancement

Noise cancellation is the process of reducing noise in a recording for the relative enhancement of a desired signal. With recordings taken from a KingAir airplane, 30dB of noise suppression was simulated for active noise cancellation with the Least Mean Squares (LMS) algorithm [18]. In the same paper, Zangi demonstrated noise cancelation in excess of 50dB with his two-sensor stochastic gradient algorithm.

Much work has also been done in the area of adaptive algorithms for speech enhancement. For speech corrupted with office noise, 30dB of SNR improvement has been demonstrated with the recursive least squares (RLS) algorithm, as well as 24dB of improvement for the fast affine projection algorithm (APA), 13.5dB for the least mean squares algorithm, and 17.1dB for normalized-LMS (NLMS) [19]. Boll and Pulsipher demonstrated a 20dB SNR improvement of a speech signal contaminated with white noise using LMS [20]. Additionally, Shenqian demonstrated 37.1dB of enhancement with his "Improved" LMS algorithm, 36.8dB with Kwong LMS, and 29.2dB with LMS, for pure tones corrupted by white noise [21].

2.3 Currently Available Systems

Despite the challenges associated with remote acoustic sensing, there are currently a multitude of systems available for military and civilian use that employ microphones for various purposes. Most, if not all, of these acoustic packages are intended for gunshot detection, since use of firearms is of concern to the police, military, and public [22]. Additionally, there have been attempts to deploy these gunshot detection systems on aircraft, including UAVs. However, no work related to audio eavesdropping onboard an airborne platform has been found in the open literature.

2.3.1 Helicopter Alert and Threat Termination (HALTT)

HALTT [23] is a project funded by the Defense Advanced Research Projects Agency (DARPA) that uses acoustic sensors to warn helicopter pilots of incoming machine-gun and small arms fire, and is intended to act as an early warning system so that countermeasures can be deployed. The system also provides the location of the incoming fire.

2.3.2 Boomerang

Boomerang [24] is one of the more advanced shot detection systems currently in use by the United States military. It consists of an acoustic array mounted atop a mast that attaches to a vehicle such as the HMMWV, and is used for detecting supersonic projectiles.

2.3.3 Low Cost Scout UAV Acoustics System (LOSAS)

SARA, Inc. has developed an acoustic sensor package that is lightweight enough to be used aboard smaller UAVs [6]. In addition to weapons fire, it is able to detect and locate heavy vehicles and other aircraft from up to 2 kilometers away. Noise interference from wind and airframe vibration is removed with proprietary mounts and windscreens [25].

2.3.4 Shot Spotter

Shot Spotter [26, 27] is a gunfire detection system that was developed for civilian use. It is designed to work in an urban environment, and is able to precisely locate gunshots despite the echoes. One notable feature of Shot Spotter is that it is able to distinguish gunshots from automobile backfire and other city noise.

2.3.5 Shot Stalker

Another UAV platform that employs a gunshot detection system is the Shot Stalker [28]. Developed by Lockheed Martin Skunkworks, the Shot Stalker is a small UAV platform that is designed to be very acoustically quiet, so that engine noise does not interfere with signal detection.

Chapter 3

Acoustic Fundamentals and Recording

The purpose of this chapter is to provide the theoretical basis for the practicality of eavesdropping aboard an airborne platform. In doing so, we address the source degradation and recording interference factors that impede the performance of acoustic arrays for remote sensing. Due to the physical nature of air as a sound medium, and the noise inherent in transducing and recording an audio signal, there exist practical limitations to eavesdropping from a distance. Expounding upon these limitations will help determine the feasibility of eavesdropping upon various noise sources.

3.1 Sound Propagation Through Atmosphere

Given the multitude of environments in which a noise source may be present (and upon which we may want to eavesdrop), an in-depth analysis of the propagation properties of various noise sources is beyond the scope of this thesis. Therefore, let us assume that the target for eavesdropping is a simple noise source, and that the UAV platform is far enough away from the source that the sound is propagating as a spherical progressive wave. Sound travels through the atmosphere as a pressure differential that essentially consists of the elastic compression and expansion of air molecules [29]. The spherical nature of the wave propagation is one source of attenuation, as the sound intensity is inversely proportional to the distance traveled squared. This phenomenon is known as the inverse square law, and is illustrated in Figure 3.1.

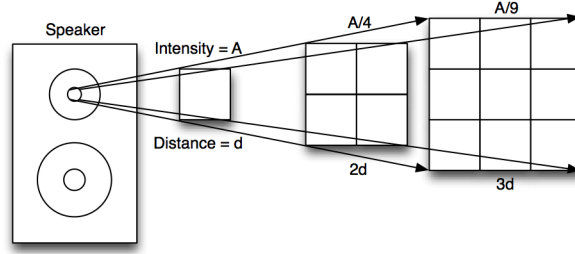


Figure 3.1: Illustration of inverse square law relation of sound intensity to distance.

Sound is classified as a longitudinal wave due to the fact that it displaces air in the direction of propagation. Sound pressure level, in decibels, is an estimate of the relative intensity of this displacement, and is calculated according to

$$L_p = 20 \log_{10} \frac{p_{rms}}{p_{ref}} \quad (3.1)$$

where L_p is the sound pressure level in decibels, p_{rms} is the sound pressure being measured, and p_{ref} is the reference sound pressure. The threshold of human hearing is $20 \mu\text{Pa}$ RMS at 1kHz [30, 31], and is used as the reference sound pressure. It should be noted that (3.1) is valid for both planar and spherical progressive waves [32]. It follows that the difference in sound pressure level between two points that are distances d_1 and d_2 apart can be calculated as

$$L_1 - L_2 = 20 \log_{10} \frac{d_2}{d_1} \quad (3.2)$$

Here, only spherical diffusion of the sound pressure is taken into account.

Other phenomenon related to the nature of the atmosphere deserve consideration when calculating the attenuation of a noise source as a function of distance, and these phenomenon are related to the elastic nature of air. Just as copper wires have an intrinsic impedance, so does air, and it is affected by factors such as temperature, pressure, and humidity. Additionally, the atmosphere attenuates high frequencies more than low, so it in effect acts like a low-pass filter of sound. Atmospheric absorption of sound is already a well-understood process, and there exist numerous resources for calculating the attenuation per unit of distance (e.g., ISO standard 9613-2:1996). The effect of

temperature and humidity on the absorption of sound in air was studied extensively by Harris [1], and Bass was responsible for deriving analytical expressions that includes the effect of pressure [33]. Plots showing atmospheric attenuation as a function of temperature and humidity are shown in Figures 3.2, 3.3, and 3.4.

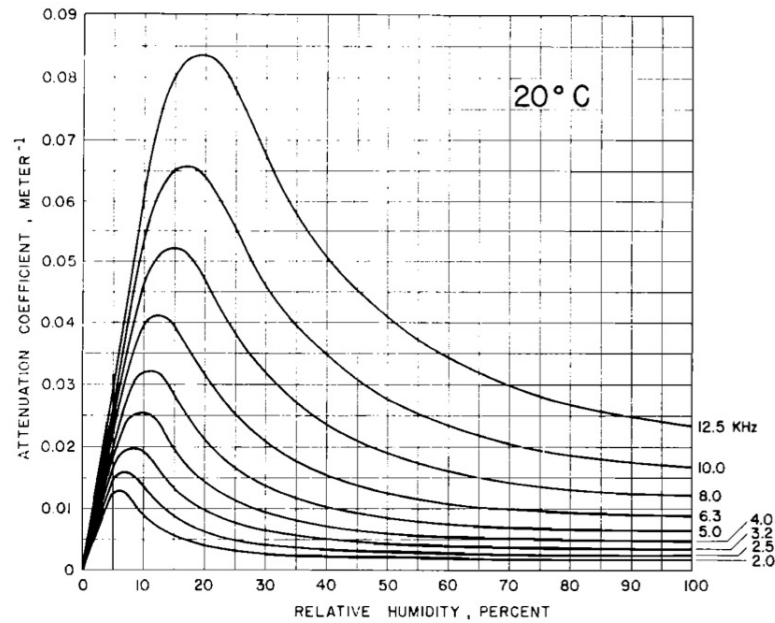


Figure 3.2: Attenuation of sound in air increases with frequency (figure from [1]).

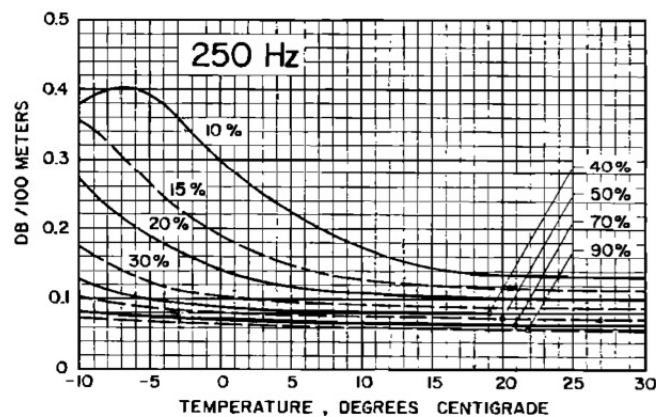


Figure 3.3: Attenuation of 250Hz sound in air decreases with increasing temperature (figure from [1]).

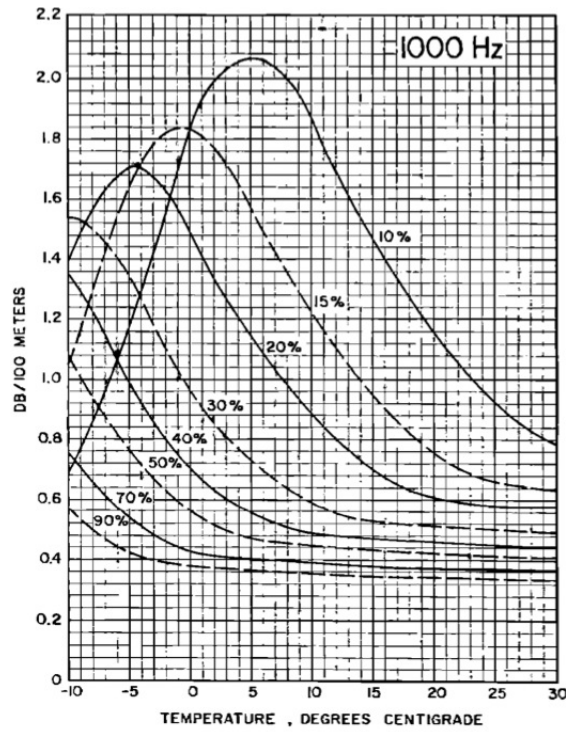


Figure 3.4: Attenuation of 1kHz sound in air decreases with increasing humidity (figure from [1]).

An additional consideration for the propagation of sound in air is the noise floor of the atmosphere. Molecules in a fluid medium undergo random perturbations due to thermal noise that is known as Brownian motion. For an ideal recording system, this thermal noise represents the absolute limit of the sensitivity of the recorder [34]. However, the magnitude of the thermal noise is at least 11dB below the best-case threshold of human hearing at any frequency [35], and as will be seen in the following section, the microphone and recorder self-noise represents the effective limit of the sensitivity of an acoustic array, not the atmospheric thermal noise.

3.2 Classification of Sound Sources

The range of human hearing is generally considered to be 20Hz-20kHz. However, this range is not necessarily the limit for an airborne acoustic sensing system. Figure 3.5 shows the range of acoustic frequencies produced by several sources, as well as the hearing range for humans, dogs, and bats.

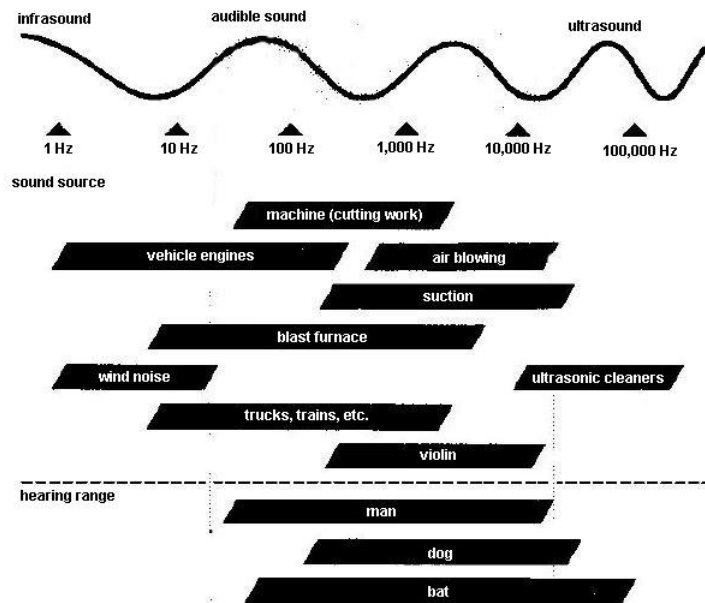


Figure 3.5: Audible frequency range and hearing range of various sources (figure from [2]).

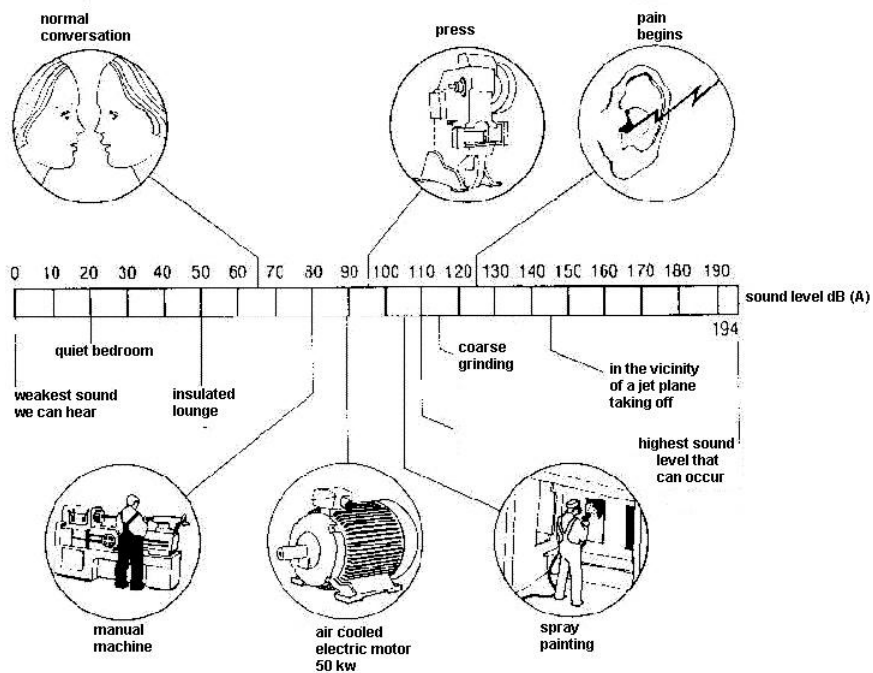


Figure 7.

Figure 3.6: Approximate intensity of various sound sources (figure from [2]).

It should be noted that audio frequencies below 200Hz and above 20kHz are known as infrasound and ultrasound, respectively. The range of audio frequencies produced by a source is an important consideration when choosing a recording system, and will be discussed in the following section.

Figure 3.6 shows the relative intensity of various noise sources. Using (3.2), we can estimate the maximum distance from which one could eavesdrop on a target. For example, Figure 3.7 shows the sound pressure level of a normal conversation, with a reference SPL of 65dB at 1 meter, as a function of distance. Assuming a noise floor of 0dB, the conversation will no longer be audible at a distance of 1778 meters, excluding atmospheric affects and barriers. Based on this calculation alone, the concept of remote acoustic sensing seems realizable.

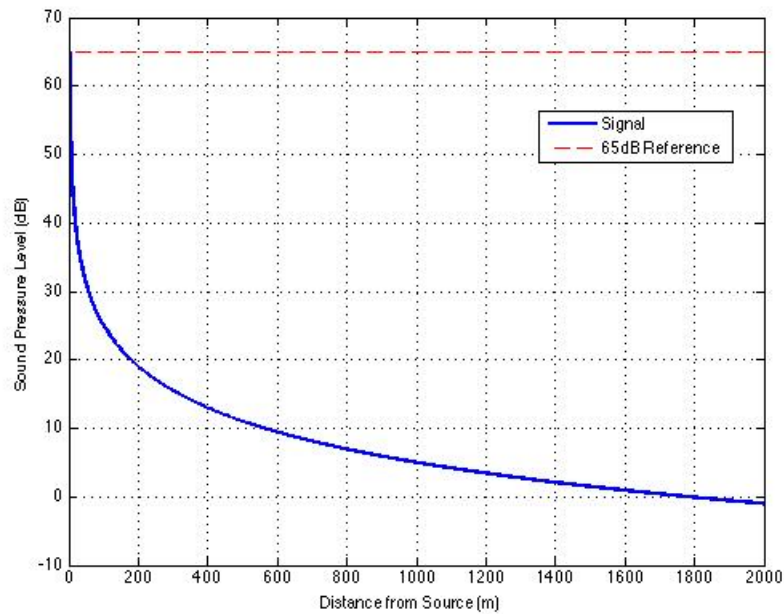


Figure 3.7: Sound pressure level of conversation, with a reference SPL of 65dB at 1 meter, as a function of distance.

3.3 Audio Recording

As mentioned in Chapter 1, the equipment used to record sound is one source of noise that will affect the performance of an airborne acoustic array. The process of digital audio recording involves the

transduction, sampling, and storing of sound waves, and the hardware typically required to perform each step includes microphones, amplifiers, and a digital sampling device.

In this section, we discuss several hardware considerations for use on an airborne platform. Choosing hardware with the proper performance characteristics can significantly reduce recording noise as a source of signal interference. As will be seen, the recording hardware is one of the limiting factors for the performance of an airborne acoustic array.

3.3.1 Audio Microphones and Preamplifiers

An audio microphone is a transducer that converts pressure differentials in the air to electrical signals. The conversion from sound to electricity is accomplished with numerous methods, and has led to a plethora of different microphone types that are currently available. A detailed discussion of the types of microphones currently available is beyond the scope of this thesis. However, it is important to understand what characteristics of microphones in general are significant to the goal of airborne acoustic recording, as these characteristics will affect the performance of the system.

A microphone preamplifier is also a necessary component of a recording system since the electrical signal generated by the microphone is often not strong enough to be processed by the recording equipment. The preamplifier provides gain for the audio signal produced by the microphone to bring it up to the line level of the recorder. The following sections describe specific considerations for the attributes of microphones and preamplifiers in terms of airborne eavesdropping.

Directionality

The design of a microphone affects its sensitivity to sound waves from various directions. Omnidirectional microphones are equally sensitive to sound pressure waves arriving from any direction, while cardioid, subcardioid, supercardioid, hypercardioid, bi-directional, and shotgun microphones are directionally dependent. The directionality of these various types of microphones are shown in the polar patterns in Figure 3.8. The benefit of using a directional microphone over an omnidirectional one is that spatial filtering is intrinsic in the former.

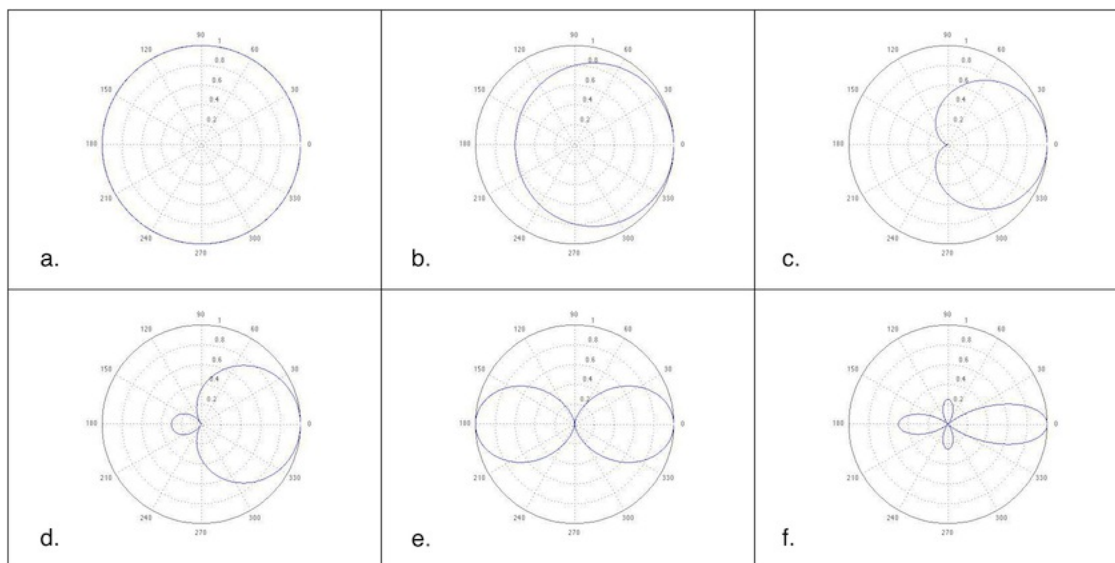


Figure 3.8: Directionality of microphone types: (a) omnidirectional; (b) subcardioid; (c) cardioid; (d) supercardioid; (e) bidirectional; (f) shotgun.

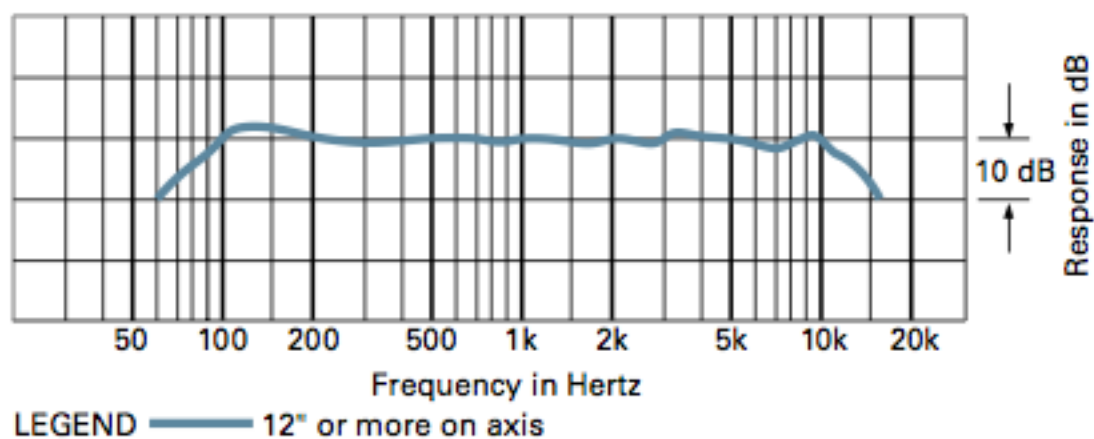


Figure 3.9: Frequency response of Audio Technica Pro 42 boundary microphone (figure from [3]).

Frequency Response

As discussed in section 3.2, the audible audio range is generally considered to be 20Hz to 20kHz. Most microphones are intended to record sound in this frequency range, but they are not equally

sensitive to all frequencies within that range. Figure 3.9 shows the frequency response of the Audio Technica Pro 42 boundary microphone [1]. As can be seen, the Pro 42 microphone attenuates sound frequencies below 100Hz, and above 10kHz, and does not have a flat response in-between. If the goal of an airborne acoustic array is accurate sound reproduction, it is necessary either to choose a microphone with a flat response curve over the frequencies of interest, or to compensate using signal processing.

Transfer Factor and Sensitivity

The transfer factor is the ratio by which sound pressure, in units of pressure (i.e., pascals), is converted to an open circuit voltage. The transfer factor is often confused with sensitivity, and the former is expressed in units of millivolts per pascal (mV/Pa). In contrast, microphone sensitivity is expressed in decibels, and is related to the transfer factor according to the following equation:

$$Sensitivity = 20 \log_{10} \left(\frac{TransferFactor}{1V/Pa} \right) [dB] \quad (3.3)$$

It should be noted that by letting $p_{ref} = 1V/Pa$, (3.3) is identical to (3.1).

Sensitivity is significant because it stipulates the output voltage of the microphone in relation to the input sound pressure level. For remote sensing, a microphone must be sensitive enough to distinguish signals, which have been attenuated over great distances, from the noise produced by the electronics.

Self Noise

Many condenser microphones incorporate a preamplifier that amplifies the signal produced by the microphone so that it is strong enough to be processed by the recording equipment. This preamp not only boosts the desired signal, but also adds the thermal noise of the electronics. The self noise is the equivalent SPL that would generate the electrical noise in the microphone, and typical values range from 40dB SPL for low quality microphones, down to -5dB SPL for very high quality ones. The self noise of a microphone is a critical consideration for recording sound from an airborne

platform, and is one of the limiting factors in how far away from a source the aircraft can effectively eavesdrop.

Maximum Input Sound Level and Dynamic Range

The maximum input sound level (MISL) is closely related to the transfer factor of a microphone. While the transfer factor is the relation between the measured sound pressure to the output line voltage, the MISL indicates the sound pressure at which the output voltage of the microphone will begin clipping. This is an important consideration for airborne acoustic sensing, as the sound level aboard a UAV must not cause saturation of the microphones of the sensor package. Additionally, the dynamic range is the difference in decibels between the MISL and the self noise.

Signal-to-Noise Ratio

The signal to noise ratio (SNR) is a well known concept in signal processing, and is the ratio of the power in the desired signal to the power in the noise. For a microphone, the self noise represents the noise in calculating the SNR, and $1Pa$ is often used as the reference signal power. The SNR is then calculated with the following:

$$\text{SNR [dB]} = 20 \log_{10} \frac{1Pa}{20\mu Pa} - N_{self} = 94dB - N_{self} \quad (3.4)$$

where N_{self} is the self noise of the microphone.

Total Harmonic Distortion

A microphone functions by converting sound tones to electrical signals. The total harmonic distortion (THD) is the ratio of the power in the harmonics of the sound tone to that of the fundamental frequency of the tone. THD can be calculated as

$$\text{THD} = \frac{\sqrt{V_2^2 + V_3^2 + \dots + V_n^2}}{V_1} \quad (3.5)$$

where V_1 is the RMS voltage of the fundamental frequency of the tone, and V_i is the i^{th} harmonic ($i > 1$). The cause of harmonic distortion depends on the type of microphone being used. In electret microphones, much of the distortion is a result of nonlinearities in the preamplifier [36]. The harmonic distortion affects how accurately a microphone can record the frequency components of the desired signal. It should be noted that the value of the MISL is often provided in terms of total harmonic distortion.

3.3.2 Audio Recorders

The purpose of the audio recorder is to sample the voltage signals produced by the microphone and preamplifier and store the sampled values in a format that is suitable for reproduction. The performance specifications of a microphone such as self noise, harmonic distortion, transfer factor, and maximum input sound level, are also considerations that must be accounted for when choosing an audio recorder that minimizes recording noise.

For the purpose of this thesis, we are limiting our discussion to digital audio recorders. Therefore, sampling theory and format are two additional considerations that must be taken into account. The following is a discussion of pertinent audio recorder specifications and how they contribute to recording noise.

Sampling Rate

In order to accurately reproduce a signal without aliasing, the sampling rate must exceed twice the highest frequency content of the signal, known as the Nyquist rate. As an example, if the signal being recorded has a maximum frequency of 10kHz, the recorder must sample at a rate of at least 20kHz in order to accurately reproduce it. As the sampling rate increases, so must the storage and processing requirements of the recorder, as well as the computational requirements for signal processing. However, there are numerous signal processing benefits to oversampling a signal, including increased resolution and white-noise reduction by averaging. Therefore, an ideal sampling rate is one that minimizes the computational requirements of the desired signal processing techniques.

Word Length

The word length is the number of bits used to digitally record the sampled audio signal, and determines the quantization error inherent in the recorder. Many of the adaptive algorithms that will be tested for this project are highly sensitive to quantization error due to the propagation of this error over many operations. The effect of quantization errors can be mitigated by increasing the word length, but this also increases the amount of storage required for the recordings and computing power to implement the signal processing. The relationship of the word length to the quantization error for linearly quantized signals is

$$-\frac{y_{max} - y_{min}}{2(L - 1)} \leq e_q(n) \leq \frac{y_{max} - y_{min}}{2(L - 1)} \quad (3.6)$$

where $e_q(n)$ is the quantization error for sample n , L is the number of quantization levels, and y_{max} and y_{min} are the maximum and minimum signal levels, respectively. It should be noted that the number of quantization levels depends upon the word length.

Chapter 4

Noise in an Airborne Environment

The final impedance factor that will affect the performance of an airborne acoustic array is environmental interference. Necessary to our study of environmental noise interference is an understanding of aeroacoustics and how noise is generated from air flow. In this chapter, we discuss some fundamentals of aeroacoustics, as well as how wind generates noise in microphones. Identifying the mechanism by which various types of aircraft noise can be generated will help to determine a suitable approach for attenuation of these sources.

The material presented in this chapter is applicable to both fixed and rotary wing UAVs. The two fixed wing aircraft, which will serve as a platform for later tests, are also introduced. Additionally, preliminary flight recordings are presented that demonstrate the magnitude of the environmental noise sources.

4.1 Environmental Noise Interference

The main goal of this project will be to filter out environmental noise while preserving a desired signal that is the target of eavesdropping. To accomplish this, we must first understand the various types of environmental noise present on an aircraft. Although all noise sources are indistinguishable to a microphone transducer, the method by which noise is generated can vary. We will elaborate

on the environmental sources of interference in Table 1.1 and discuss the various mechanisms by which unwanted sound is generated.

4.1.1 Wind Noise

Wind is the flow of air caused by pressure differentials in the atmosphere and is classified as either laminar or turbulent flow. Laminar flow is the uniform motion of air in a parallel direction, while turbulent flow is the random mixing motion of air particles. The distinction between these types of wind flow is shown in Figure 4.1.

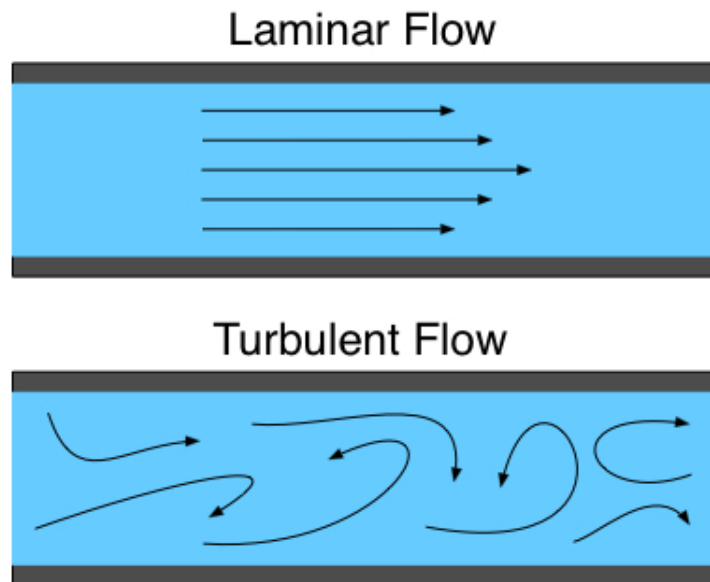


Figure 4.1: Comparison of turbulent and laminar fluid flow.

Turbulence is caused by either temperature fluctuations in the atmosphere (e.g., solar heating), or the interaction of wind with physical bodies [37]. These types of turbulence are known as convective and mechanical, respectively, and mechanical turbulence is the mechanism by which air flow generates sound. Although a detailed discussion of aircraft aeroacoustics is beyond the scope of this thesis, it is worth noting that when airflow is interrupted by an obstacle, sound is generated [38].

It should be noted that the mechanism by which sound is generated from unsteady fluid flow is

different from the noise generated by microphones in the presence of airflow. Morgan and Raspet [39] demonstrated that laminar and turbulent flows generate noise by different means. For laminar flow, the fluctuating wake of the microphone causes velocity changes in the transducer, which are interpreted as pressure variations. In the case of turbulent flow, they showed that pressure fluctuations picked up by the microphone are caused by velocity changes in the turbulence.

As mentioned in Chapter 1, a single microphone cannot distinguish between wind noise and acoustic pressure due to sound propagation. However, since fluid flow due to wind propagates slower than sound, it is possible to distinguish between wind noise and the signal of interest by using a microphone array. Shields [40] demonstrated that wind noise recorded by each element of a microphone array is correlated up to certain frequencies when the separation between microphones is small enough. This notion will be important in the next chapter when discussing adaptive noise cancellation.

4.1.2 Aircraft Noise

Aircraft aeroacoustics is the study of the noise produced by an airplane in flight. As discussed in section 4.1.1, noise is generated by perturbed airflow, and both the propulsion method and aircraft aerodynamics can cause this interruption. Therefore, the aircraft propulsion system, boundary layer flow, and actuation and control machinery all generate noise. Additionally, air interacting with the surface of the aircraft—as well as unbalanced propulsion and machinery—can induce vibration in the airframe. Additional information on aeroacoustic noise sources can be found in [41].

It is worth noting that sources of environmental noise onboard an aircraft can be classified into two types: radiative sources and transfer sources. The former type includes all aeroacoustic sources that generate sound. The latter, transfer sources, includes all environmental noise sources that affect the microphone transducer, but do not propagate at the speed of sound. Categorization of the environmental noise sources is further expanded in Table 4.1.

Table 4.1: Sources of aircraft environmental noise.

Type	Factor
Radiative Sources	Propulsion Noise Boundary Layer Flow Actuation and Control
Transfer Sources	Aircraft Vibration Airflow Over Microphone(s)

4.2 Airborne Test Platforms

The airborne test platforms used for the experiments in this thesis are two radio-controlled fixed-wing aircraft. The following sections present the technical specifications of the aircraft, and discuss the noise profile for each.

4.2.1 Super Cub Test Platform

The Super Cub LP RTF (model #HBZ7300), produced by HobbyZone, is an electric aircraft that uses a brushed DC motor [42]. The fuselage and wings of the Super Cub are constructed of Styrofoam, and can carry a payload of 7 ounces. A stock photo of the Super Cub is shown in Figure 4.2.



Figure 4.2: Super Cub LP RTF RC Airplane [4]

Given the 7 ounce payload capacity of the Super Cub, it is not suitable for flight testing with a recording payload, and is only used for ground tests in a laboratory. The technical specifications of the Super Cub are provided in Table 4.2.

Table 4.2: Super Cub LP RTF specifications.

Wingspan	47.7 in
Overall Length	32.5 in
Flying Weight	25.2 oz
Engine	4800 Brushed DC
Propeller Size	9×6
Radio	27MHz 3-Channel Proportional
Landing Gear	Fixed Main with Steerable Tail Wheel
Throttle	Proportional - 34 Settings
Control Surfaces	Elevator, Rudder
Flap Servo	Power HD 7150MG
Transmitter Range	2500 ft

4.2.2 Monocoupe Test Platform

The test platform used for flight testing is a Super Craft Monocoupe 90A 1/4 scale [43], produced by Kangke Industrial USA, Inc. The Monocoupe is a balsa wood, radio controlled aircraft, powered by a gasoline engine. A photo of the Monocoupe 90A is shown in Figure 4.3.

The Monocoupe is powerful enough to carry a payload of two microphones and a recording device, and is flown by an experienced RC pilot who was generous enough to make it available. One advantage of the Monocoupe is that its skin is a wind-proof covering called Oracover that *provides little attenuation of external sound*. Additionally, the aircraft has a large fuselage that can accommodate several cubic feet of equipment. Figure 4.4 shows the inside of the fuselage of the Monocoupe. The technical specifications of the Monocoupe used for this experiment are in Table 4.3.



Figure 4.3: Super Kraft Monocoupe 90A RC airplane.



Figure 4.4: Access panel for fuselage of Monocoupe 90A.

Table 4.3: Kangke Monocoupe 1/4 scale specifications.

Wingspan	96.5 in
Overall Length	61.5 in
Flying Weight	13-14.5 lb
Engine	DLE-30 Gasoline
Propeller	Xoar 18×10
Controller	Futuba 7C 2.4GHz
Receiver	Futuba R617FS
Throttle Servo	Futuba S3004
Rudder Servo	Futuba S9201
Flap Servo	Power HD 7150MG
Elevator Servo	Futuba S9201
Aileron Servo	Futuba S3004

Acoustic Analysis of Monocoupe Test Platform

Application of suitable signal processing techniques for reduction of environmental noise requires a careful analysis of the noise generated by the Monocoupe under power. In order to characterize the aircraft acoustically, a recording is made of the Monocoupe in flight. The test setup is provided in Chapter 6. The frequency spectrum of the recording, created using Audacity 1.3.14 and a Hanning window of length 16384, is shown in Figure 4.5.

As can be seen, the majority of the frequency content of the noise produced by the Monocoupe is below 1kHz, with a peak of -26dB at 125Hz. The frequency content above 1kHz decreases steadily at a rate of approximately 1.0dB/kHz. Additionally, Figure 4.6 shows a spectrogram of the the frequency content of the recording between 0 and 24kHz using a Hanning window of length 4096. The non-stationary nature of the noise produced by the Monocoupe is evident in the spectrogram, and will effect the choice of signal processing techniques to remove the unwanted environmental noise.

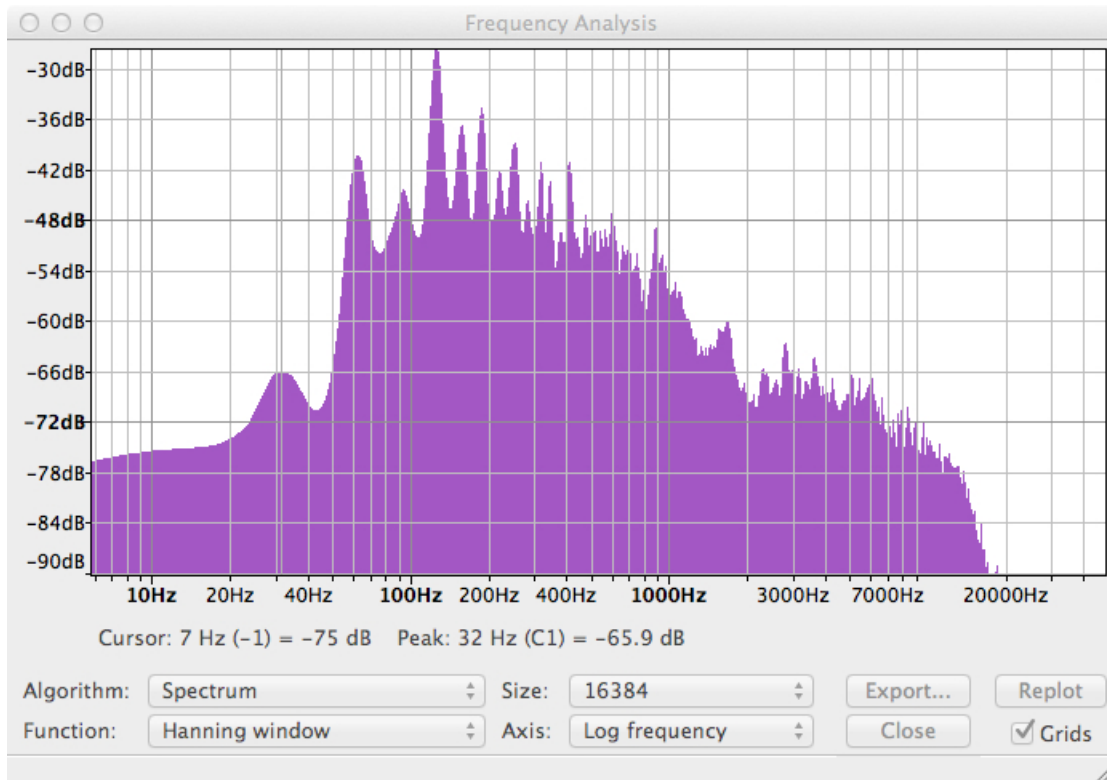


Figure 4.5: Sound spectrum of moncoupe in-flight (Relative Intensity (dB) vs. Frequency (Hz)).

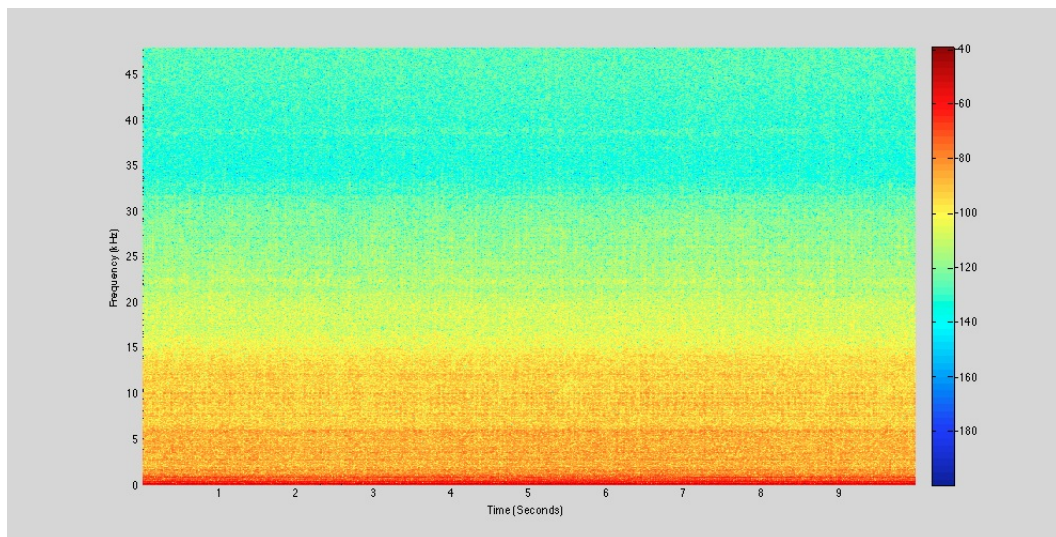


Figure 4.6: Spectrogram of Moncoupe in-flight using a Hanning window of length 4096 (Frequency (kHz) vs. Time (s)).

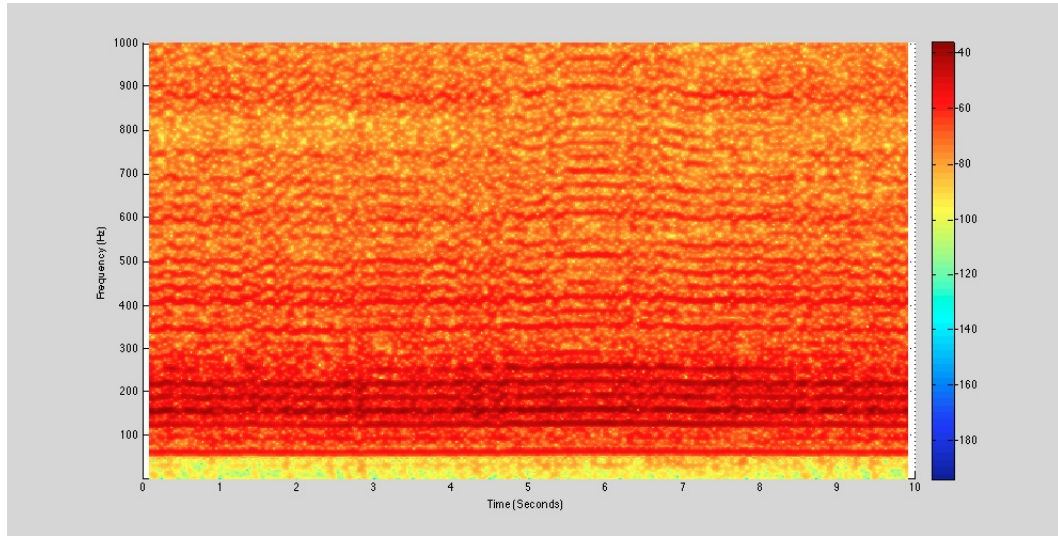


Figure 4.7: Spectral bands produced by Monocoupe engine using a Hanning window of length 16384 (Frequency (Hz) vs. Time (s)).

Lastly, Figure 4.7 shows the spectral lines in the Monocoupe recording that are indicative of an internal combustion engine. The spectrogram uses a Hanning window of length 16384 in order to provide greater frequency resolution. The bands below 300Hz are particularly strong and are responsible for the peak in the spectrum shown in Figure 4.5.

Chapter 5

Adaptive Noise Cancellation

The three types of acoustic interference that will degrade the performance of an airborne acoustic sensor are source degradation, recorder interference, and environmental noise. Although there is little that can be done to control source degradation (other than increase the gain of the recording device), recorder interference can be minimized by designing a system with flat frequency response and low self noise. For the radiative and transfer sources of environmental interference produced by wind, aeroacoustics, and the aircraft control and propulsion, we propose the use of adaptive noise cancellation techniques.

As discussed in Chapter 2, adaptive noise cancellation is an effective technique for removal of unwanted environmental noise, and although beamforming may be more effective for noise suppression in a specific direction, the latter will actually increase the wind and environmental noise in the main lobe. In the following sections, we discuss the fundamentals of adaptive noise cancellation, and present three adaptive algorithms that were tested for airborne eavesdropping.

5.1 Fundamentals of Adaptive Noise Cancellation

Figure 5.1 shows the basic problem of adaptive noise cancellation. A desired signal $s(n)$ is corrupted with uncorrelated noise $v(n)$, and recorded by a primary microphone. A secondary microphone records noise source $u(n)$ that is related to $v(n)$ by the transfer function $G(z)$. The distance

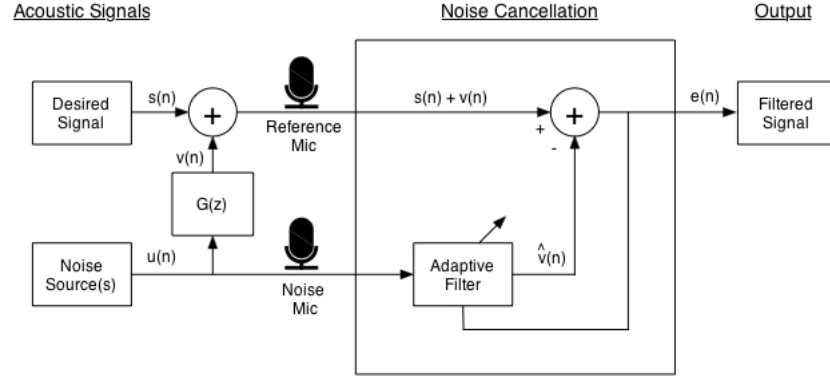


Figure 5.1: Block diagram of generic adaptive noise cancellation concept.

between the two microphones, difference in frequency responses of the microphones, and other unknown factors contribute to the transfer function.

The purpose of the adaptive filter is to estimate the transfer function, $G(z)$, by some means, so that $u(n)$ can be filtered to produce a signal, $\hat{v}(n)$, that is as close a replica as possible of $v(n)$. The filtered noise is then subtracted from $s(n) + v(n)$ to obtain an estimate of the desired signal, $e(n)$ —which is both the output of the system and the error signal used to adapt the filter. Adaptation of the filter is required because $G(z)$ is not fixed [12]. From Figure 5.1, we obtain the following equation.

$$e(n) = s(n) + v(n) - \hat{v}(n) \quad (5.1)$$

Some practical considerations for implementation of adaptive noise cancellation include the number, placement, and isolation of the microphones. An adaptive noise canceling setup can include multiple microphones for both the noise and reference signal, but the microphones must be placed to ensure there is no delay in the recorded noise components. In order for $\hat{v}(n)$ to be an accurate estimate of $v(n)$, the noise in each signal must be correlated. As seen in Chapter 5, all environmental sources of noise interference, including wind, are correlated with proper microphone placement. Additionally, since the filtered noise is subtracted from the reference signal, it is important to isolate the noise microphone so that it detects little of the desired signal, as leakage can degrade the performance of the filter. The effect of leakage of the desired signal into the noise recording was studied by Widrow

[12].

The setup for the experiment in this thesis utilizes two microphones: a noise microphone and a reference microphone. The signal recorded by the reference microphone will contain the unwanted wind and UAV noise listed in Table 4.1, as well as the desired signal that is acquired through eavesdropping. The signal recorded by the noise microphone should contain only the unwanted wind and UAV noise. One of the challenges is to then isolate the noise and reference microphones so that the signal of interest is contained only in the latter.

5.2 Adaptive Algorithms

The first issue that needs to be addressed is an explanation of the reason for using adaptive algorithms. As the diagram in Figure 5.1 shows, a transfer function ($G(z)$) exists between the noise recorded by the two microphones. Assuming $G(z)$ is stationary and known, it should be possible to determine the transfer function using optimal techniques such as a Wiener filter. However, due to aircraft vibration and other unknown phenomenon, the transfer function between the two microphones will vary with time.

Adaptation is also needed to determine the transfer function between the noise and reference microphones. Optimal techniques such as Wiener filtering assume the autocorrelation and cross-correlation of the two recorded signals is known. When they are not known, the autocorrelation and cross-correlation must be estimated from the samples, making the Wiener filter sub-optimal.

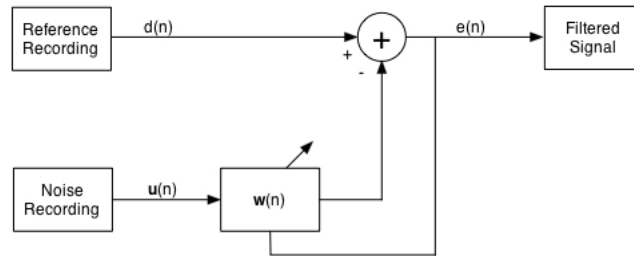


Figure 5.2: Block diagram of generic adaptive filter.

A diagram of the noise cancellation setup with a generic adaptive filter is shown in Figure 5.2.

There, $\mathbf{u}(n)$ is a vector of length M , containing recorded values of $u(n)$ from time n to $n - M + 1$, $d(n)$ is the reference recording ($d(n) = s(n) + v(n)$), and $\mathbf{w}(n)$ is a finite impulse response filter of length M that is adapted using the filtered signal, $e(n)$. For this thesis, a bold lowercase letter denotes a vector, while bold uppercase letters are used for matrices. Lowercase letters that are not bold denote scalar values. Using (5.1) and Figure 5.2, we obtain

$$e(n) = d(n) - \mathbf{w}^T(n)\mathbf{u}(n) \quad (5.2)$$

where the superscript T denotes the transpose.

Numerous adaptive algorithms have been developed that differ by how $e(n)$ is used to optimize the filter, and several variations may exist for each algorithm. The following is a list of characteristics that describe the performance of adaptive filters [44]:

- **Rate of convergence:** The speed at which a filter converges to the optimal Wiener solution.
- **Mis-adjustment:** The deviation of the filter from the Wiener solution.
- **Tracking:** Effectiveness of the filter in a non-stationary environment.
- **Robustness:** Error performance of the filter in handling small disturbances.
- **Computational requirements:** Hardware requirements for implementation of the algorithm.
- **Structure:** Determines how the filter can be implemented.
- **Numerical properties:** Sensitivity of the filter to quantization error.

The process of filter adaptation functions by minimizing a cost function related to the input signals to the filter. The filtered signal, $e(n)$, is then used for feedback for the adaptation process and to tune the filter. For this experiment, we propose to test the effectiveness of the following adaptive algorithms at removal of unwanted environmental noise:

- **Least Mean Squares (LMS)**
- **Affine Projection (AP)**
- **Extended Recursive Least Squares Type-1 (ERLS-1)**

Table 5.1: Comparative performance of LMS, AP, and ERLS-1 adaptive filters.

	Convergence Speed	Misadjustment	Tracking Performance	Computational Requirements
Best	ERLS-1	ERLS-1	LMS	LMS
	AP	AP	AP	AP
Worst	LMS	LMS	ERLS-1	ERLS-1

The algorithms listed above were chosen because they are representative of the performance spectrum of adaptive filters, and because their performance characteristics for noise cancellation and signal enhancement are known for other applications (see Chapter 2). Additionally, each algorithm minimizes the same cost function: the output power of the error signal, $e(n)$. The comparative performance characteristics are provided in Table 5.1, and will be expounded upon in the following sections.

For noise cancellation, the metric used to evaluate the performance of each filter is the signal to noise ratio improvement. For a wide sense stationary signal, the sample signal to noise ratio is computed with the following:

$$\text{SNR [dB]} = 10 \log_{10} \frac{E\{s^2(n)\}}{E\{v^2(n)\}} \quad (5.3)$$

In the case of non-stationary signals (see Section 4.2.1), (5.3) serves as an estimate of the SNR. The SNR improvement is then the difference in the SNR of the desired signal before and after filtering.

The metric used to determine the performance of a filter for signal enhancement is the mean squared error (MSE). The MSE provides a means of quantifying the difference between the actual signal and the filtered result, and is calculated as

$$MSE(\hat{\theta}) = E\{(\hat{\theta} - \theta)^2\} \quad (5.4)$$

where θ and $\hat{\theta}$ are the actual and estimated parameters, respectively.

It should be noted that numerous modifications exist that serve to improve upon one or more

of the performance characteristics of each algorithm, but we restrict ourselves to implementing the time-domain transverse form of each filter in the setup shown in Figure 5.2. Each of the filters utilized for this project are implemented in Matlab for the purpose of filtering the recorded data, and the code for each filter is provided in Appendix A. We expound upon the characteristics and implementation of each filter in the following subsections.

5.2.1 Least Mean Squares Algorithm

The LMS filter was originally conceived by Widrow and Hoff at Stanford University in 1959 [45]. As Widrow and Hoff's derivation shows, the algorithm performs by minimizing the output error using the stochastic gradient method. The main benefit of the LMS algorithm is low computational requirements at the expense of performance.

The tracking performance of LMS has been analyzed extensively by Eleftheriou and Falconer [46], Marcos and Macchi [47], and Hajivandi and Gardner [48], as well as Haykin [44]. Additionally, Rupp investigated the tracking performance of LMS for periodically time-varying systems [49]. The convergence rate of LMS can be tuned by using the parameter μ , and the convergence properties of the algorithm are detailed in [50]. Below is a summary of the LMS algorithm.

Summary of Least Mean Squares Algorithm

Parameters:

M - Filter length

μ - Step-size parameter

$\mathbf{u}(n)$ - M -by-1 input vector at time n (Noise mic)

$d(n)$ - Desired response (Reference Mic)

$e(n)$ - Filter output / error value

Initialization:

$\mathbf{w}(0) = 0$

$n = 1$

Filtering Loop:

$$1) e(n) = d(n) - \mathbf{w}^T(n-1)\mathbf{u}(n)$$

$$2) \mathbf{w}(n) = \mathbf{w}(n-1) + \mu\mathbf{u}(n)e(n)$$

3) Increment n and restart loop

5.2.2 Affine Projection Algorithm

The affine projection algorithm is an extension of the well-known normalized least mean squares filter, and was proposed by Ozeki [51]. The APA uses the method of Lagrange multipliers to minimize the output error subject to the constraint that changes in the filter weights must be attenuated, which is known as the *principle of minimal disturbance* [44]. At the expense of higher computation complexity, the APA filters offers faster convergence than LMS, and performance comparable to the RLS algorithm. Below is a summary of the APA.

Summary of Affine Projection Algorithm

Parameters:

M - Filter length

N - Filter order

μ - Adaptation parameter

δ - Regularization parameter

$\mathbf{u}(n)$ - M -by-1 input vector at time n (Noise mic)

$d(n)$ - Desired response (Reference Mic)

$\mathbf{e}(n)$ - N -by-1 filter error vector

$e(n)$ - Filter output / error value

I - Identity Matrix

Initialization:

$\mathbf{w}(0) = M$ -by-1 zero vector

$n = 1$

Filtering Loop:

- 1) $\mathbf{A}^T(n) = [\mathbf{u}(n), \mathbf{u}(n-1), \dots, \mathbf{u}(n-N+1)]$
- 2) $\mathbf{d}^T = [d(n), d(n-1), \dots, d(n-N+1)]$
- 3) $\mathbf{e}(n) = \mathbf{d}(n) - \mathbf{A}(n)\mathbf{w}(n-1)$
- 4) $\mathbf{w}(n) = \mathbf{w}(n-1) + \mu\mathbf{A}^T(n)(\mathbf{A}(n)\mathbf{A}^T(n) + \delta I)^{-1}\mathbf{e}(n)$
- 5) $e(n) = d(n) - \mathbf{w}^T(n)\mathbf{u}(n)$
- 6) Increment n and restart loop

5.2.3 Extended Recursive Least Squares Type-1 Algorithm

The RLS algorithm is touted as the ultimate adaptive filter with regards to rate of convergence and mis-adjustment. However, this performance comes at the cost of significantly increased computational complexity. In terms of operation, the RLS is analogous to that of a Kalman filter, wherein the extended RLS Type-1 algorithm includes a process noise term in order to improve tracking performance. Due to poor performance of the RLS filter in initial tests, the ERLS-1 version is used for this experiment. A derivation of the ERLS-1 algorithm can be found in [44]. Below is a summary of the ERLS-1 algorithm.

Summary of Extended Recursive Least Squares Type-1 Algorithm

Parameters:

- M - Filter length
- a - Adaptation parameter
- q - Process noise variance parameter
- $\mathbf{u}(n)$ - M -by-1 input vector at time n (Noise mic)
- $d(n)$ - Desired response (Reference Mic)
- $e(n)$ - Filter output / error value

Initialization:

$$\mathbf{w}(0) = 0$$

$$\mathbf{P}(0) = I \text{ (Identity Matrix)}$$

$$n = 1$$

Filtering Loop:

$$1) \pi(n) = \mathbf{P}(n-1)\mathbf{u}(n)$$

$$2) \mathbf{k}(n) = \frac{a\pi(n)}{\lambda + \mathbf{u}^T(n)\pi(n)}$$

$$3) e(n) = d(n) - \mathbf{w}^T(n-1)\mathbf{u}(n)$$

$$4) \mathbf{w}(n) = a\mathbf{w}(n-1) + \mathbf{k}(n)e(n)$$

$$5) \mathbf{P}(n) = \mathbf{P}(n-1) - \frac{\pi(n)\mathbf{u}^T(n)\mathbf{P}(n-1)}{\mathbf{u}^T(n)\pi(n) + 1}$$

$$5) \mathbf{P}(n) = a^2\mathbf{P}(n) + q\mathbf{I}$$

7) Increment n and restart loop

Chapter 6

Experimental Validation of Effectiveness of Adaptive Algorithms

In order to validate the effectiveness of the adaptive algorithms listed in Chapter 5, an experiment is devised to capture the environmental noise onboard an airplane in flight. The Super Kraft Monocoupe 90A described in Chapter 4 is used as the testbed for the experiment. The motivation for the experiment, test plan, preliminary experiments, flight-test setup, and results are provided in the following sections. A detailed analysis of the performance of the algorithms for noise cancellation and signal enhancement is also provided.

6.1 Preliminary Experiments

The purpose of this thesis is to validate the effectiveness of adaptive algorithms at attenuation of environmental noise that is recorded aboard an aircraft, in-flight. For this goal, a series of experiments were devised to gain understanding of adaptive noise cancellation, determine which variables affect the performance of the filters, and find a suitable platform for a flight test. The experiments performed with each aircraft, as well as the results, are provided in Tables [6.1](#) and [6.2](#).

Experiments 1 through 6 were preliminary—but necessary—for the final flight test. This is because experiments 1-3 were performed to gain better understanding of the adaptive algorithms,

while experiments 4-6 were necessary to determine a suitable test platform and recording package. Experiment 7 was the final flight test, and a detailed test plan is provided in the following sections.

Table 6.1: Preliminary experiments with Super Cub test platform.

Experiment	Result
1) In-Lab Test #1	Verified function of matlab programs which implement adaptive algorithms. Verified that performance of adaptive algorithms agree with results in literature.
2) Anechoic Test	Determined that recording environment affects filter length for adaptive algorithms.
3) In-Lab Test #2	Determined optimal microphone placement to increase performance of adaptive filters.
4) Flight Test	Determined Super Cub unable to carry microphone package.

Table 6.2: Flight tests with Monocoupe test platform.

Experiment	Result
5) Flight Test #1	Microphones came loose during flight.
6) Flight Test #2	Microphones were placed close to engine and clipping occurred, two 10dB Dayton Audio attenuators were added to recorder package after experiment.
7) Flight Test #3	A 7 minute 38 second recording was made that was used for analysis.

6.2 Flight Test Setup

The following experiment was devised that implements the two microphone adaptive noise cancellation setup described in Chapter 5 to test the effectiveness of the LMS, AP, and ERLS-1 algorithms for noise cancellation and signal enhancement. The Super Kraft Monocoupe 90A serves as the platform for the ANC system, and in-flight recordings of the environmental noise are made in order to capture the environmental noise generated by the aircraft. The effectiveness of the aforementioned adaptive filters are then tested on the recording.

Before the experiment, it was determined that eavesdropping would not be attempted due to the limited equipment that was available. Instead, recordings of the environmental noise would be made in-flight, and an artificially generated signal would be added to the reference recording. Adding a generated signal would allow for the best-case-scenario of 100% microphone isolation, and would make it possible to control the signal-to-noise ratio of the desired signal to the environmental noise.

As seen in the previous chapter, the noise cancellation algorithms used for this experiment require two microphones. Therefore, a recording device capable of simultaneously recording two channels is necessary. Additionally, it is necessary to measure the speed of the aircraft in order to correlate the velocity to the intensity of the noise being generated. Lastly, since weather can affect the propagation of sound, a weather meter is used to record pertinent environmental parameters. The following materials and equipment are used for the experiment.

Equipment List -

- 1. RC Airplane:** Super Kraft Monocoupe 90A 1/4 Scale (Described in Chapter 4)
- 2. Recorder:** Tascam DR-40 with Firmware Version 1.00
- 3. Microphones:** Two Audio Technica Pro-42 Boundary Condenser Microphones
- 4. Attenuators:** Two Dayton Audio XATT10 XLR 10dB Attenuators
- 5. Weather Meter:** Kestrel 4000 with Firmware Version 4.02
- 6. GPS:** Holux M-241 Logger
- 7. Timer:** Burberry Men's BU7715 Watch
- 8. Adhesives:** Industrial Strength Velcro and Scotch Outdoor Mounting Tape

The attenuators are necessary for the experiment because the noise from the aircraft saturated the recording device on the minimum gain setting. It should be noted that for each microphone, the case and protective grating is removed in order to minimize any differences in manufacturing. Therefore, the condenser elements are exposed to the interior of the fuselage. The microphones and attenuators are attached to the recorder as shown in Figure 6.1.

The Audio Technica Pro-42 microphones were chosen because they are lightweight, have low self noise, and are compatible with the phantom power provided by the Tascam recorder. The mi-



Figure 6.1: Recording device setup.

crophones are placed so that there were no obstructions between either condenser element. The microphone condenser elements are placed next to each other in order to minimize the delay between noise sources in each recorded signal. However, the metal edges of the microphones are placed approximately 1mm apart in order to ensure they did not make contact. The placement of the microphones is shown in Figure 6.2.

It should be noted that the placement of the microphones is a result of trial and error. The microphones are placed internally because even slight wind noise will cause saturation. This eliminated airflow over the microphone as a transfer source of environmental noise. The microphone placement shown in Figure 6.2 also ensures that they will not interfere with the operation of the aircraft.

Prior to the experiment, the self noise of the recording system is measured by placing the package shown in Figure 6.1 in an anechoic chamber. The package is allowed to record in the chamber for several minutes in the absence of external noise sources. Using these recordings, the self noise of the recorder package is determined to have a variance of approximately $3 \times 10^{-9} V^2$, and a noise floor of approximately -110dB (using a Hanning window of length 16384). From Figure 4.5, it is evident that the noise produced by the Monocoupe in-flight is well above the noise floor of

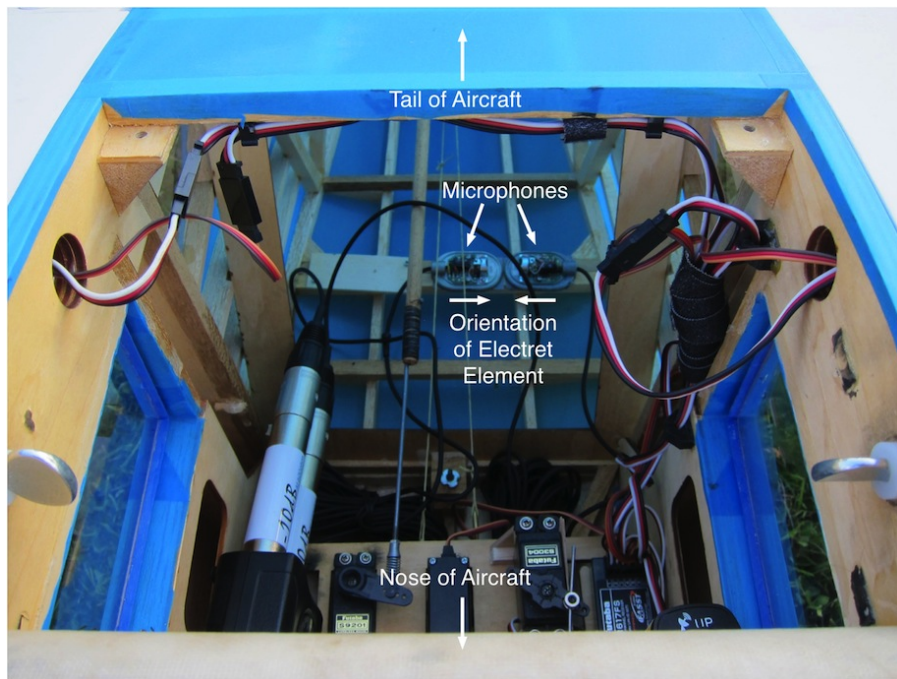


Figure 6.2: Placement of the microphones within Monocoupe chassis.

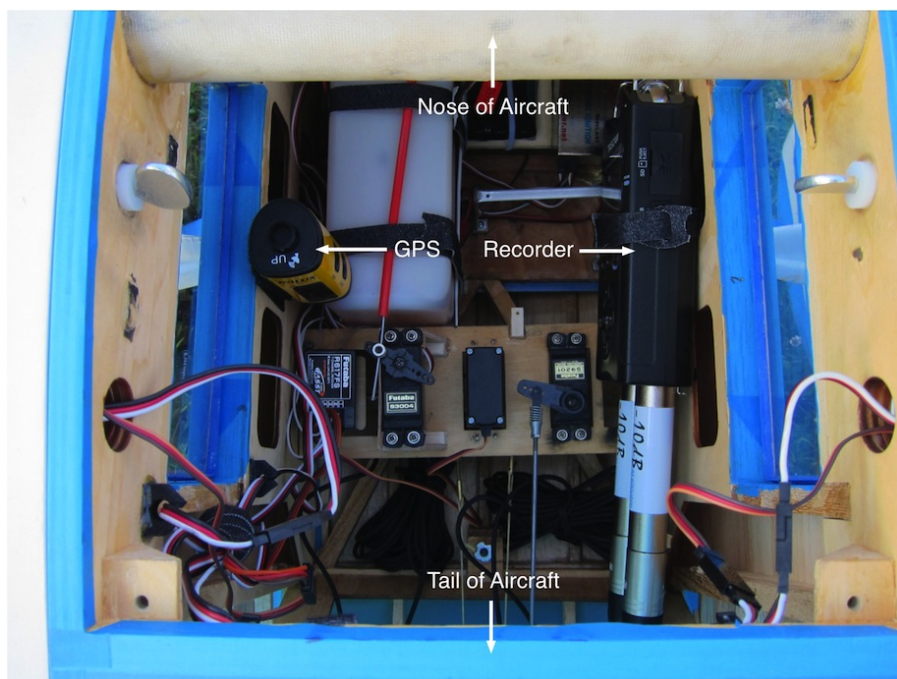


Figure 6.3: Placement of the recorder and GPS within Monocoupe chassis.

the recorder.

The GPS unit used for tracking the speed and altitude of the aircraft must be oriented properly in order to function. The GPS unit is affixed to the inside of the chassis with velcro (hook side attached to the wood), so that it is oriented right-side up. Lastly, the recorder and attenuators are strapped inside the chassis with velcro. The orientation and placement of the GPS and recorder within the Monocoupe airframe is shown in Figure 6.3.

Before performing this experiment, a survey was made of the available multi-channel handheld recorders. The performance of the available recorders is limited when compared to conventional audio recording equipment in regards to word length, sampling frequency, and recording formats. The Tascam DR-40 is adequate for this experiment because it can provide power for external microphones. The following settings were used for the recording format:

Recorder Settings -

- 1. Format:** 24-bit Floating Point WAV File
- 2. Sampling Rate:** 96kHz
- 3. Low Cut:** Off
- 4. Pre Record:** Off
- 5. Auto Record:** Off
- 6. Record Mode:** Stereo
- 7. Source:** External Input 1/2 (Mic + Phantom)
- 8. MS Decode:** Off
- 9. Phantom Power Input Gain Level:** Zero (0)
- 10. Peak Reduction:** Off

The waveform audio file format—or WAV, after its filename extension—is a standard for recording and storing audio, and is used as the format for this experiment. The WAV format quantizes analog audio signals using linear pulse code modulation (LPCM), meaning that the difference between successive quantization levels is constant. WAV files can be encoded as either fixed point or

floating point numbers. In order to reduce quantization error, the latter is preferred since floating point numbers offer higher resolution. It should also be noted that WAV is a lossless method of storing audio.

6.3 Flight Test

The experiment was performed on Friday, May 25, at 3:00PM at the Miami RC flying field in Xenia, Ohio. An expert pilot volunteered his time to fly the instrumented aircraft. Before the experiment, the following weather measurements were made with the Kestrel 4000 by resetting the Min/Max/Avg memory and recording for one minute:

Weather Measurements (Average)-

1. **Wind Speed:** 295 fpm Average; 335 fpm Maximum
2. **Temperature:** 31.0°C
3. **Pressure:** 988.0hPa
4. **Humidity:** 49.1%

The recorder, microphones, and GPS were placed in the aircraft as shown in Figures 6.2 and 6.3. The timer, audio recorder, and GPS recorder were started at the same time to synchronize the recordings. The aircraft engine was then started, and allowed to idle for two minutes in order to warm up. Upon flying the aircraft, the pilot admitted no noticeable difference in flight characteristics with the recording equipment onboard. The total recording time for the experiment was 7 minutes and 38 seconds, and the following maneuvers were performed:

Maneuvers -

1. Idling - 00:00
2. Takeoff - 01:47
3. One pass to determine flight readiness - 01:57

4. Low altitude passes at slow and high speed - 02:47
5. High altitude pass at slow and high speed - 05:32
6. Landing - 06:39
7. Taxiing

The time at which each maneuver was performed, after start, is listed in MM:SS format. The flight path and altitude and velocity data are shown in Figures 6.4 and 6.5, respectively.



Figure 6.4: Recorded flight path for experiment with second of latitude/longitude lines in pink

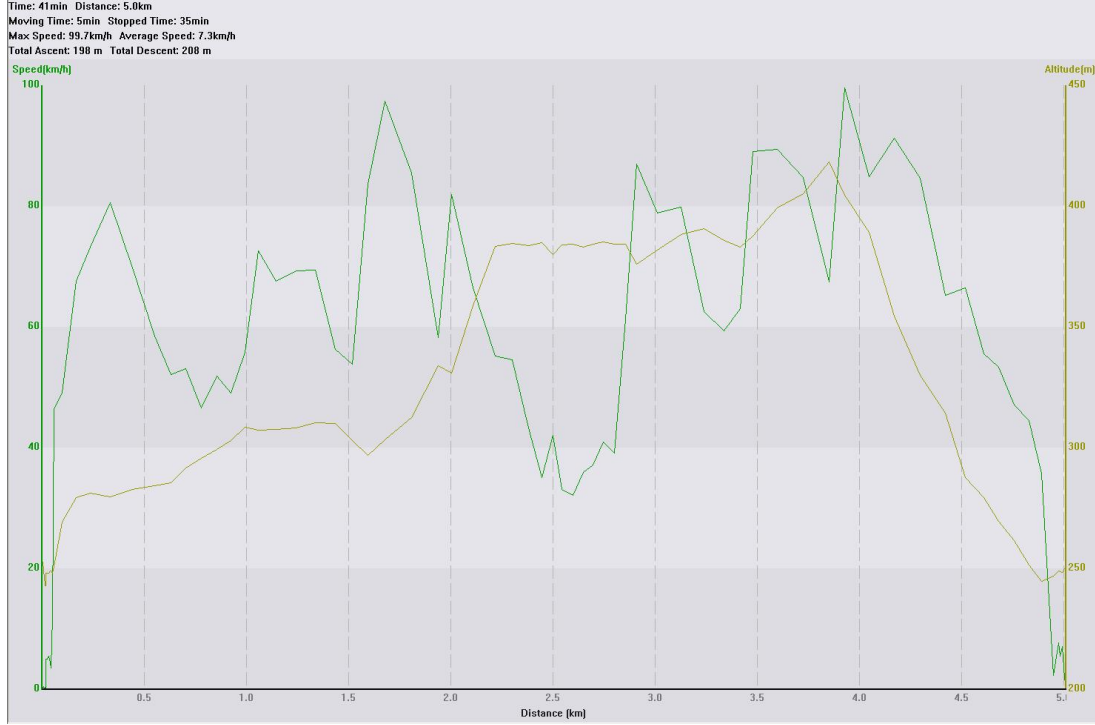


Figure 6.5: Recorded altitude (above sea level) and velocity during experiment.

6.4 Analysis

In the following sections, we present the analysis of the effectiveness of the adaptive algorithms discussed in Chapter 5 at removal of the unwanted environmental noise recorded during the experiment. In order to determine a baseline for signal enhancement, the noise cancellation performance of the filters is first measured. A chirp signal is then generated and added to the reference recording at various SNR values in order to test the filters.

6.4.1 Noise Cancellation

For the analysis of the noise cancellation performance of the LMS, APA, and ERLS-1 filters, three sections of the recording made during the experiment are used. The difference between each recording is the speed at which the aircraft was traveling. The recordings used for this analysis are as follows:

Recordings for Analysis -

1. High Speed (Greater than 80km/hr): 3:25 to 3:35
2. Cruising Speed (Approximately 40km/hr): 4:13 to 4:23
3. Low Speed (Less than 40km/hr): 6:25 to 6:35

The recordings listed above are used as inputs for the Matlab programs provided in Appendix A. Since the recordings were made in stereo, the second track serves as the reference input. The filters are tuned by incrementally increasing or decreasing the parameters, and using (5.3) to determine the effect on performance. Adjusting the parameters is a tradeoff between mis-adjustment and robustness: smaller adaptation and step size parameters make the filter more robust to perturbations in the inputs, while larger values improve the mis-adjustment. Since the filter length and convergence rate must be taken into account, only the last nine seconds of each recording is used to calculate the SNR improvement. Tables 6.3 and 6.4 provide the values of the tunable parameters used for each filter, as well as performance of the algorithms for each of the recordings.

Table 6.3: Values of tunable parameters for LMS, APA, and ERLS-1 filters for noise cancellation by recording.

Adaptation	Parameter	Filter Parameters by Recording		
		High Speed	Cruise Speed	Low Speed
LMS	Filter Length - M	12000	12000	12000
	μ	0.07	0.02	0.0057
APA	Filter Length - M	400	400	400
	Filter Order - N	10	10	10
	μ	0.95	0.95	0.95
	δ	1×10^{-12}	1×10^{-12}	1×10^{-12}
ERLS-1	Filter Length - M	400	400	400
	a	0.999	0.999	0.999
	q	1000	1000	1000

Table 6.4: Performance of LMS, APA, and ERLS-1 filters for noise cancellation.

Adaptation	Noise Reduction for Recording [dB]		
	High Speed	Cruise Speed	Low Speed
LMS	23.5	26.3	29.2
APA	33.7	33.4	37.0
ERLS-1	27.7	28.1	33.1

Due to the computational requirements of the ERLS-1 algorithm, the filter length was not increased beyond 400. With the parameters listed in Table 6.3, the execution time of the ERLS-1 algorithm was 1.5 hours on a 15” Macbook Pro with an Intel Core i7 2675QM processor. Increasing the filter length beyond 400 yielded little improvement and it was prohibitively time-consuming to fine tune the parameters.

As shown in Table 6.4, the AP algorithm outperforms the LMS and ERLS-1 algorithms for noise cancellation. It is also apparent that the performance of the filters is degraded as the speed of the aircraft increases. With the exception of the cruise and high speed recordings for APA, the filter performance decreases monotonically as the speed increases. However, it is not known if this is caused by increased wind noise or aircraft vibration due to the engine.

6.4.2 Signal Enhancement for Additive Chirp

In order to test the effectiveness of the LMS, AP, and ERLS-1 algorithms at signal enhancement, it is necessary to add a signal to the recordings that will serve as a simulated target of eavesdropping. Not wanting to limit the analysis to a specific type of recording, a chirp is generated using Audacity version 1.3.14 that serves as the simulated signal of interest. The following parameters are used for the chirp generator:

Chirp Generator Parameters -

- 1. Waveform:** Sine
- 2. Frequency Start-End:** 20Hz - 10kHz
- 3. Amplitude Start-End:** 0.1 - 0.1
- 4. Interpolation:** Linear
- 5. Duration:** 9 seconds

The chirp is then exported to a 32-bit floating point WAV file so that it can be added to the aircraft recordings. Using Matlab, both the recordings and the chirp are imported, and the latter is added to the second track by summation. By adjusting the amplitude of the chirp, the SNR can be controlled. Given that the variance of a sinusoid of amplitude A is $\frac{A^2}{2}$, and using (5.3), we can calculate the amplitude of the chirp that will provide the desired SNR with

$$A = \sqrt{2(\sigma_d^2)(10^{\frac{SNR[dB]}{10}})} \quad (6.1)$$

where $SNR[dB]$ is the desired signal to noise ratio, in decibels, and σ_d^2 is the variance of the signal to which the chirp is being added.

Since the performance of the filters is comparable at different speed, the cruise speed recording is used for signal enhancement and the 9-second chirp is added after the first second of the recording. Three recordings are produced that have chirp SNR values of -10dB, -20dB, and -30dB. Figure 6.6 shows a spectrogram of the reference signal of the Cruise Speed recording with the added -20dB chirp, and the relative intensity of the spectral content of the respective chirps are shown in Table 6.5. The three recordings are then filtered and the parameter values are adjusted by increasing SNR improvement until there is noticeable distortion of the filtered chirp. The MSE of the filtered signal for each algorithm, as well as the calculated SNR improvement, is provided in Table 6.6 and 6.7, respectively. The filter parameter values associated with each recording are listed in table 6.8.

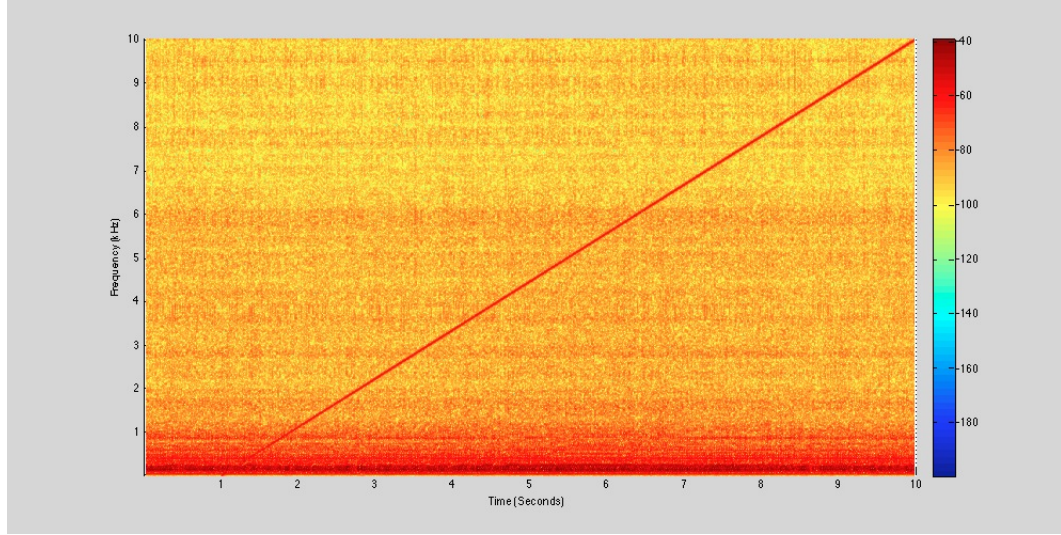


Figure 6.6: Spectrogram of reference signal of low-speed recording with 9-second chirp and SNR=-20dB using a Hanning window of length 4096 (Frequency [kHz] vs. Time [s]).

Table 6.5: Relative of spectral content of scaled chirps using Hanning window of length 16384.

	Relative Spectral Magnitude [dB]
-10dB Chirp	-63
-20dB Chirp	-72
-30dB Chirp	-82

Table 6.6: MSE of LMS, APA, and ERLS-1 filters for signal enhancement with additive chirp.

Adaptation	MSE		
	-10dB Chirp	-20dB Chirp	-30dB Chirp
LMS	1.09×10^{-4}	5.10×10^{-5}	2.11×10^{-5}
APA	1.09×10^{-4}	4.07×10^{-5}	1.57×10^{-5}
ERLS-1	1.19×10^{-4}	5.09×10^{-5}	2.97×10^{-5}
Chirp Variance	2.75×10^{-4}	2.53×10^{-5}	2.53×10^{-6}

Table 6.7: SNR improvement of NLMS, APA, and RLS filters for signal enhancement with additive chirp.

Adaptation	SNR Improvement [dB]		
	-10dB Chirp	-20dB Chirp	-30dB Chirp
LMS	14.0	17.0	20.8
APA	14.0	17.9	22.1
ERLS-1	13.6	15.9	19.1

Table 6.8: Values of tunable parameters for LMS, APA, and ERLS-1 filters for signal enhancement by recording.

Adaptation	Parameter	Filter Parameters by Recording		
		-10dB Chirp	-20dB Chirp	-30dB Chirp
LMS	Filter Length - M	12000	12000	12000
	μ	0.0015	0.0025	0.007
APA	Filter Length - M	4000	4000	4000
	Filter Order - N	2	2	2
	μ	0.06	0.1	0.3
	δ	1×10^{-12}	1×10^{-12}	1×10^{-12}
ERLS-1	Filter Length - M	400	400	400
	a	0.999	0.999	0.999
	q	0.04	0.06	0.1

As seen in Table 6.6, the performance results of the filters for signal enhancement is similar to that of noise cancellation. The affine projection algorithm provides the lowest MSE, followed by ERLS-1 and LMS. For the -20dB chirp, the signal is readily visible in the spectrogram of the result of the LMS filtered shown in Figure 6.7. Comparing Figures 6.8, 6.9, and 6.10 to Figure 4.5, the filters provide approximately 30dB of attenuation of the noise below 600Hz. Additionally, the noise above 10kHz is attenuated by approximately 3dB.

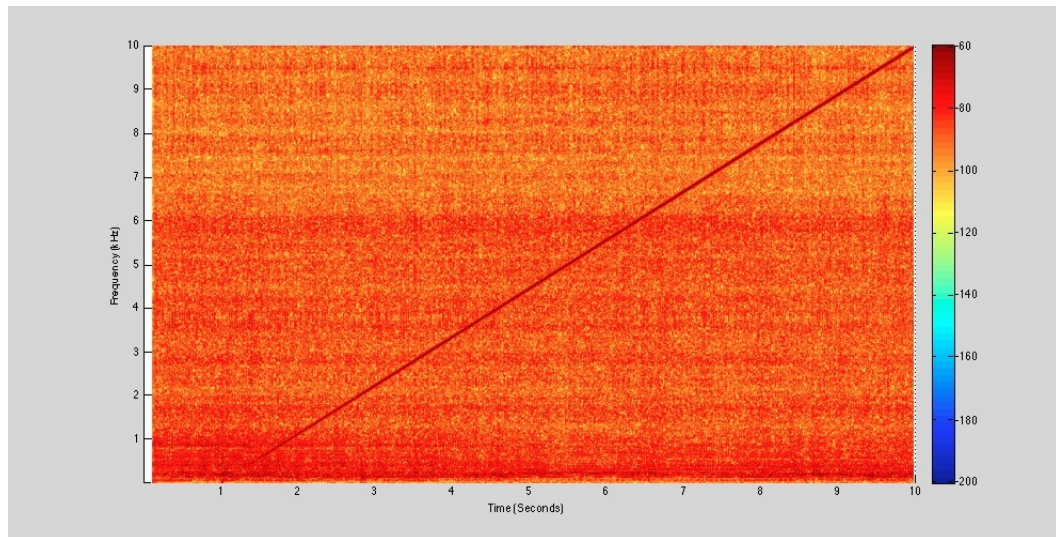


Figure 6.7: Spectrogram (using Hanning window of length 4096) of cruise speed recording with -20dB chirp, filtered with LMS (Frequency [kHz] vs Time [s]).

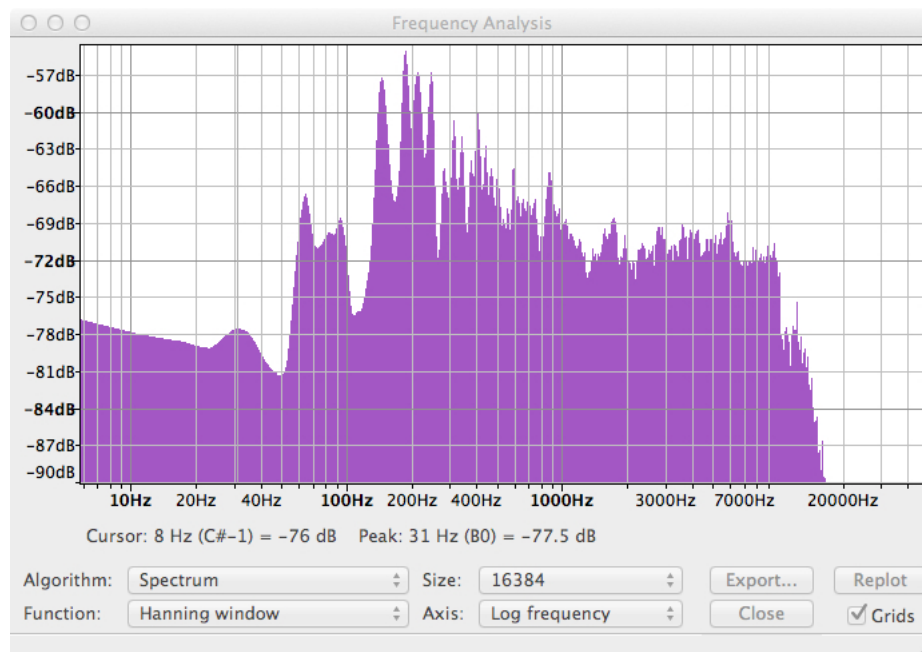


Figure 6.8: Spectrum of cruise speed recording with -20dB chirp, filtered with LMS.

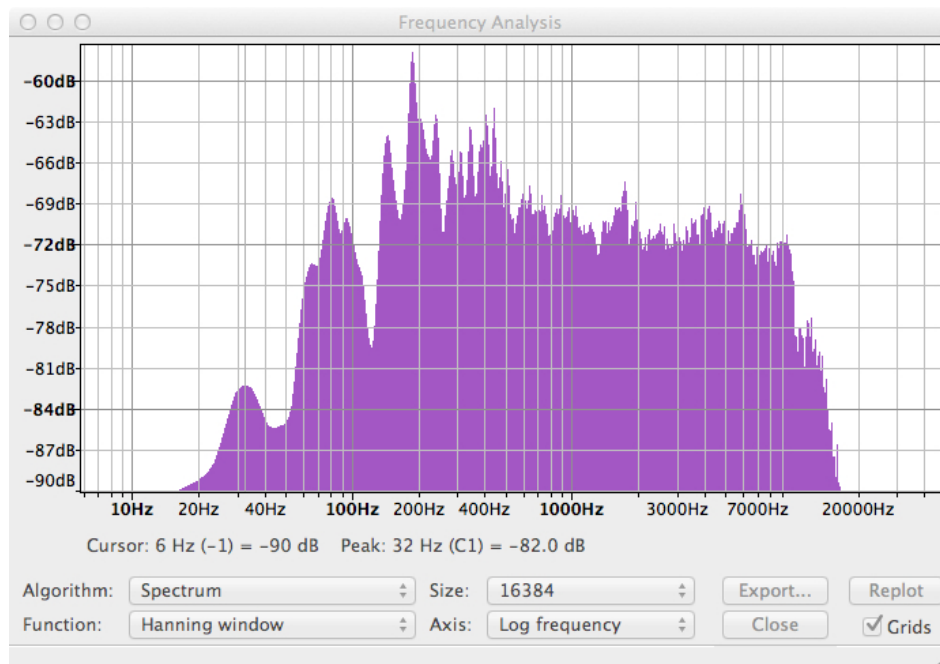


Figure 6.9: Spectrum of cruise speed recording with -20dB chirp, filtered with APA.

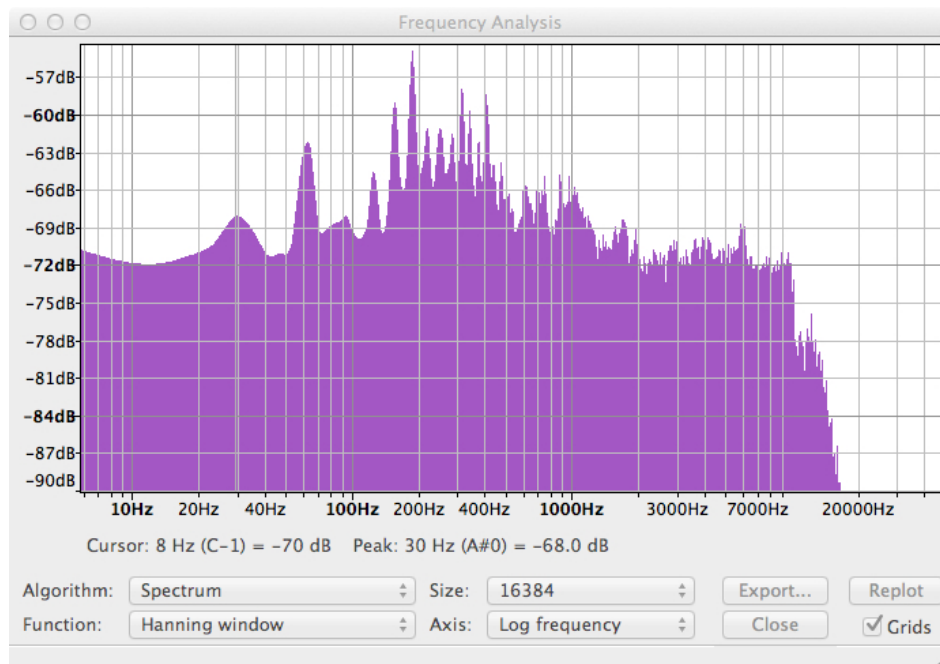


Figure 6.10: Spectrum of cruise speed recording with -20dB chirp, filtered with ERLS-1.

Chapter 7

Conclusion

Ground and marine-based acoustic arrays are used for a myriad of applications in order to locate and identify sources of noise. The benefit of using microphone arrays onboard an airborne platform are the ability to track a target and a wider coverage area. However, due to the limited propagation of sound through the atmosphere and the noisy environment onboard an aircraft, there are serious obstacles that must be overcome before an airborne array can be adopted for the same roles as ground and marine-based sensors.

In this thesis, we discuss the numerous factors that impede the performance of an airborne acoustic array. Currently available methods for attenuating these factors are presented, and the use of adaptive algorithms for cancellation of environmental noise is proposed. The effectiveness of the least mean squares, affine projection, and extended recursive least squares algorithms for reduction of unwanted wind and aircraft noise is tested. An experiment is performed wherein a recording is made onboard an RC aircraft in-flight, and the data is used to evaluate the performance of the algorithms for noise cancellation and signal enhancement of an added chirp.

The results of the experiment demonstrate that adaptive algorithms are effective at reducing unwanted aircraft and wind noise and enhancing a desired signal. However, more effective algorithms are warranted in order to discern a signal of interest at lower frequencies due to interference from engine noise. Despite the numerous sources of acoustic interference aboard an aircraft, effective techniques are available for attenuating these sources, and the goal of employing an acoustic

array aboard an airborne platform is realizable. With the addition of adaptive noise cancellation, the following compensation techniques are available:

Table 7.1: Techniques for mitigation of impedance factors of airborne acoustic sensors.

Type	Mitigation Technique
Source Degradation	Increased Signal Gain
Recording Interference	Low Noise / Distortion Recorder
Environmental Interference	Windscreen Muffler Aeroacoustic Improvements Vibration Dampening Mount Beamforming Adaptive Noise Cancellation

Future work to evaluate the effectiveness of adaptive algorithms for signal enhancement aboard an airborne platform would involve utilizing more advanced noise canceling techniques. For example, fast versions of the AP and RLS algorithms that allow for longer filter lengths with lower computational requirements may improve performance. Additionally, filter variants with adaptive parameters may increase the SNR improvement while lowering MSE. Any future work involving a more advanced acoustic array package should also involve the use of system identification techniques to determine optimal filter orders for the adaptive algorithms. Both autoregressive and moving-average modeling could be used since infinite impulse response adaptive filters may be more effective random noise sources aboard an aircraft [52].

Appendix A

Matlab Code for Adaptive Algorithms

A.1 Normalized Least Mean Squares Program

```
%%  
% function e = LMSFilterIt(n,d,fs)  
% written by -      Ryan Fuller  
% organization -    AFRL / RBCCX  
% version -        1.0  
% date -           6 October, 2011  
%  
% description - function e = LMSFilterIt(n,d,fs) uses the Normalized Least  
% Mean Square algorithm to filter the unwanted noise from the reference  
% signal, d, by using the noise signal, n. Argument 'fs' is the sampling  
% frequency of the recordings. The function produces the filtered output,  
% e.  
%  
%%  
function [e,h] = LMSFilterIt(n,d,fs)  
  
% Set default sampling rate  
if nargin < 3  
    fs = 96000;
```

```

end

tic

% Parameters
p = 12000; % filter order
disp(['Filter length = ' num2str(p)])
mu = 0.02; % step size

% Initialization
h = zeros(p,1); % filter coefficients
e = n*0; % filter output

for m = p:length(d)

    % Acquire chunk of data
    x = n(m:-1:m-p+1);

    % Calculate error
    e(m) = d(m)-h'*x;

    % Update filter coefficients
    h = h + (mu*e(m)*x)/(x'*x);

end

toc

% Plot it!
t = linspace(0,length(d)/fs,length(d));
figure;
plot(t,d,t,e);
xlabel('Time (s)');
legend('Reference', 'Filtered', 'Location', 'NorthEast');

% Calculate SNR improvement

```

```

SNRi = 10*log10(var(d)/var(e));

disp([num2str(SNRi) 'dB SNR Improvement'])

return

```

A.2 Affine Projection Program

```

%%
% function y = APFilterIt(n,d,fs)
% written by -      Ryan Fuller
% organization -    AFRL / RBCCX
% version -         1.0
% date -            6 October, 2011
%
% description - function y = APFilterIt(n,d,fs) uses the Affine Projection
% algorithm to remove the unwanted noise from the reference signal, d,
% using the noise signal, n. Argument 'fs' is the sampling frequency of the
% recordings. The function produces the filtered output, y.
%
%%
function y = APFilterIt(n,d,fs)

% Set default sampling rate
if nargin < 3
    fs = 96000;
end

tic

% Parameters
M      = 400; % input length
N      = 10;  % filter order
mu     = 0.95; % step size

```

```

delta    = 1.0e-12*eye(N);

% Initialization
w        = zeros(M,1); % filter coefficients
e        = zeros(N,length(n)); % filter error
A        = zeros(N,M);

for m = N+M:length(d)

    % Acquire next chunk of data
    for i = 1:N
        A(i,:) = n(m-i+1:-1:m-(i+M)+2)';
    end

    % Calculate error
    e(:,m) = d(m:-1:m-N+1)-A*w;

    % Update filter coefficients
    w = w + mu*A'/(A*A'+delta)*e(:,m);

    % Filter output
    y(m) = d(m) - w'*n(m:-1:m-M+1);

end

toc

% Plot it!
t = linspace(0,length(d)/fs,length(d));
figure;
plot(t,d,t,y);
xlabel('Time (s)');
legend('Reference', 'Filtered', 'Location', 'NorthEast');

% Calculate SNR improvement
SNRi = 10*log10(var(d(1:end))/var(y(1:end)));

```

```
disp([num2str(SNRi) 'dB SNR Improvement'])
```

```
return
```

A.3 Extended Recursive Least Squares Type-1 Program

```
%%
% function e = ERLSFilterIt(n,x,fs)
% written by -      Ryan Fuller
% organization -    AFRL / RBCCX
% version -         1.0
% date -            26 October, 2011
%
% description - function e = ERLSFilterIt(n,d,fs) uses the Extended
% Recursive Least Square Type-1 algorithm (Haykin,"Adaptive Filter Theory",
% 2002) algorithm to remove the unwanted noise from the reference signal,
% x, using the noise signal, n. Argument 'fs' is the sampling frequency of
% the recordings. The function produces the filtered output, e.
%
%%
function e = ERLSFilterIt(n,x,fs)

% Set default sampling rate
if nargin < 3
    fs = 96000;
end

tic

% Parameters
p    = 400;                % filter order
a    = 0.999;              % forgetting factor
q    = 1000.0;             % variance
```

```

% Initialization
w = zeros(p,1);           % filter coefficients
P = q*eye(p);             % inverse correlation matrix
I = eye(p);
e = x*0;                  % error signal

for m = p:length(x)

    % Acquire chunk of data
    y = n(m:-1:m-p+1);

    % Parameters for efficiency
    Pi = P*y;

    % Filter gain vector update
    k = (a*Pi)*inv(y'*Pi + 1);

    % Error signal equation
    e(m) = x(m) - w'*y;

    % Filter coefficients adaption
    w = a*w + k*e(m);

    % Inverse correlation matrix update
    P = P - (Pi*y'*P)/(y'*Pi);
    P = a^2*P + q*I;

    % Counter to display progress of filter
    if mod(m,1000) == 0
        disp([num2str(m/1000) ' of ' num2str(floor(length(x)/1000))])
    end

end

toc

```

```

% Plot it!
t = linspace(0,length(x)/fs,length(x));
figure;
plot(t,x,t,e);
title('Result of ERLS Filter')
xlabel('Time (s)');
legend('Reference', 'Filtered', 'Location', 'NorthEast');

% Calculate SNR improvement
SNRi = 10*log10(var(x)/var(e));

disp([num2str(SNRi) 'dB SNR Improvement'])

return

```

Bibliography

- [1] C. M. Harris, "Absorption of sound in air versus humidity and temperature," *The Journal of the Acoustical Society of America*, vol. 40, no. 1, pp. 148–159, 1966. [Online]. Available: <http://link.aip.org/link/?JAS/40/148/1>
- [2] [Online]. Available: <http://www.safeworkaustralia.gov.au/sites/SWA/SafetyInYourWorkplace/HazardsAndSafetyIssues/NoiseAndHearing/Pages/NoiseControl.aspx>
- [3] Pro 42 cardioid condenser boundary microphone. [Online]. Available: http://www.audio-technica.com/cms/resource_library/literature/dfd10558d61908f9/pro42_submit.pdf
- [4] (2012) Super cub lp rtf images. [Online]. Available: <http://secure.hobbyzone.com/catalog/hz/HBZ7300.html?media=image>
- [5] P. Marmaroli, X. Falourd, and H. Lissek, "A uav motor denoising technique to improve localization of surrounding noisy aircrafts: proof of concept for anti-collision systems," 2012.
- [6] B. Kaushik, D. Nance, and K. Ahuja, "A review of the role of acoustic sensors in the modern battlefield," in *11 th AIAA/CEAS Aeroacoustics Conference(26 th Aeroacoustics Conference)*, 2005, pp. 1–13.
- [7] H. Hubbard, "Aeroacoustics of flight vehicles: Theory and practice. volume 2. noise control," DTIC Document, Tech. Rep., 1991.
- [8] W. E. Prather, D. H. Bridges, T. Edwards, and D. S. Thompson, "Capabilities study of

- airborne acoustic sensor arrays,” E. M. Carapezza, Ed., vol. 6562, no. 1. SPIE, 2007, p. 656209. [Online]. Available: <http://link.aip.org/link/?PSI/6562/656209/1>
- [9] D. Wilson, R. Greenfield, and M. White, “Spatial structure of low-frequency wind noise,” *The Journal of the Acoustical Society of America*, vol. 122, no. 6, pp. EL223–EL228, 2007.
- [10] J. Hileman, Z. Spakovszky, M. Drela, and M. Sargeant, “Airframe design for “silent aircraft,”” *AIAA paper*, vol. 453, p. 2007, 2007.
- [11] D. Lockard and G. Lilley, “The airframe noise reduction challenge,” *NASA/TM*, vol. 213013, 2004.
- [12] B. Widrow, J. Glover Jr, J. McCool, J. Kaunitz, C. Williams, R. Hearn, J. Zeidler, E. Dong Jr, and R. Goodlin, “Adaptive noise cancelling: Principles and applications,” *Proceedings of the IEEE*, vol. 63, no. 12, pp. 1692–1716, 1975.
- [13] B. Van Veen and K. Buckley, “Beamforming: A versatile approach to spatial filtering,” *ASSP Magazine, IEEE*, vol. 5, no. 2, pp. 4–24, 1988.
- [14] R. J. Lustberg, “Acoustic beamforming using microphone arrays,” Master of Science, Massachusetts Institute of Technology, June 1993.
- [15] J. Li and H. Chen, “Least squares frequency invariant beamforming robust against microphone mismatches,” in *Information Science and Technology (ICIST), 2011 International Conference on*. IEEE, 2011, pp. 496–499.
- [16] Y. Kaneda and J. Ohga, “Adaptive microphone-array system for noise reduction,” *Acoustics, Speech and Signal Processing, IEEE Transactions on*, vol. 34, no. 6, pp. 1391–1400, 1986.
- [17] K. Farrell, R. Mammone, and J. Flanagan, “Beamforming microphone arrays for speech enhancement,” in *Acoustics, Speech, and Signal Processing, 1992. ICASSP-92., 1992 IEEE International Conference on*, vol. 1. IEEE, 1992, pp. 285–288.

- [18] K. Zangi, "A new two-sensor active noise cancellation algorithm," in *Acoustics, Speech, and Signal Processing, 1993. ICASSP-93., 1993 IEEE International Conference on*, vol. 2, April 1993, pp. 351–354 vol.2.
- [19] N. Sonbolestan and S. Hadei, "A fast affine projection algorithm based on matching pursuit in adaptive noise cancellation for speech enhancement," in *Intelligent Systems, Modelling and Simulation (ISMS), 2010 International Conference on*. IEEE, 2010, pp. 193–198.
- [20] S. Boll and D. Pulsipher, "Suppression of acoustic noise in speech using two microphone adaptive noise cancellation," *Acoustics, Speech and Signal Processing, IEEE Transactions on*, vol. 28, no. 6, pp. 752–753, 1980.
- [21] M. Shengqian, X. Guowei, M. Zhifeng, W. Shuping, and F. Manhong, "Research on adaptive noise canceller of an improvement lms algorithm," in *Electronics, Communications and Control (ICECC), 2011 International Conference on*. IEEE, 2011, pp. 1611–1614.
- [22] R. Maher, "Acoustical characterization of gunshots," in *Signal Processing Applications for Public Security and Forensics, 2007. SAFE'07. IEEE Workshop on*. IET, 2007, pp. 1–5.
- [23] D. Miles. (2010, August) New threat detection capabilities ready to test. [Online]. Available: <http://www.defense.gov/news/newsarticle.aspx?id=60458>
- [24] G. Ratnam. (2005, February) Boomerang system sweeps for snipers. [Online]. Available: <http://www.armytimes.com/legacy/new/0-ARMYPAPER-620646.php>
- [25] (2012) Sara, inc. [Online]. Available: http://www.sara.com/ISR/acoustic_sensing/LOSAS.html
- [26] R. Showen, "Operational gunshot location system," in *Proc. SPIE*, A. T. DePersia, S. Yeager, and S. M. Ortiz, Eds., vol. 2935, no. 1. SPIE, 1997, pp. 130–139. [Online]. Available: <http://link.aip.org/link/?PSI/2935/130/1>
- [27] (2012, February) The critical first step in stopping gun violence, from the world leader in gunshot detection. [Online]. Available: <http://www.shotspotter.com/sites/default/files/flex-brochure.pdf>

- [28] *Lockheed Martin Begins Production of 'Shot Stalker' UAV*, May 2010. [Online]. Available: <http://www.shotspotter.com/es/node/103>
- [29] R. Wiley and D. Richards, "Physical constraints on acoustic communication in the atmosphere: implications for the evolution of animal vocalizations," *Behavioral Ecology and Sociobiology*, vol. 3, no. 1, pp. 69–94, 1978.
- [30] H. Fletcher, "Loudness, its definition, measurement and calculation," *Jour. Acous. Soc. Amen*, p. 377, 1933.
- [31] D. Robinson and R. Dadson, "A re-determination of the equal-loudness relations for pure tones," *British Journal of Applied Physics*, vol. 7, p. 166, 1956.
- [32] L. Kinsler, A. Frey, A. Coppens, and J. Sanders, *Fundamentals of Acoustics*. Wiley, 1982.
- [33] H. Bass, H. Bauer, and L. Evans, "Atmospheric absorption of sound: Analytical expressions," *The Journal of the Acoustical Society of America*, vol. 52, p. 821, 1972.
- [34] R. Mellen, "The thermal-noise limit in the detection of underwater acoustic signals," *The Journal of the Acoustical Society of America*, vol. 24, p. 478, 1952.
- [35] F. Hunt, "Notes on the exact equations governing the propagation of sound in fluids," *J. Acoust. Soc. Am*, vol. 27, no. 6, p. 1019, 1955.
- [36] M. Taher and Abuelma'atti, "Harmonic distortion in electret microphones," *Applied Acoustics*, vol. 34, no. 1, pp. 1 – 6, 1991. [Online]. Available: <http://www.sciencedirect.com/science/article/pii/0003682X9190042D>
- [37] K. Walker and M. Hedlin, "A review of wind-noise reduction methodologies," *Infrasound Monitoring for Atmospheric Studies*, pp. 141–182, 2010.
- [38] D. Crighton, "Basic principles of aerodynamic noise generation," *Progress in Aerospace Sciences*, vol. 16, no. 1, pp. 31–96, 1975.

- [39] S. Morgan and R. Raspet, "Investigation of the mechanisms of low-frequency wind noise generation outdoors," *The Journal of the Acoustical Society of America*, vol. 92, p. 1180, 1992.
- [40] F. Shields, "Low-frequency wind noise correlation in microphone arrays," *The Journal of the Acoustical Society of America*, vol. 117, p. 3489, 2005.
- [41] H. Hubbard, "Aeroacoustics of flight vehicles: Theory and practice. volume 1. noise sources," DTIC Document, Tech. Rep., 1991.
- [42] (2012) Super cub lp rtf. [Online]. Available: <http://secure.hobbyzone.com/HBZ7300.html>
- [43] *Super Kraft Monocoupe 90A Assembly Manual*, Kangke Industrial USA, Inc., 65 East Jefryn Blvd., Deer Park, New York 11729. [Online]. Available: www.kangkeusa.com/instructions/Monocoupe%202ND.pdf
- [44] S. Haykin, *Adaptive Filter Theory*. Upper Saddle River, New Jersey 07458: Prentice Hall, Inc., 2002.
- [45] B. Widrow, M. Hoff, and S. U. C. S. E. LABS., "Adaptive switching circuits." *Defense Technical Information Center*, 1960.
- [46] E. Eleftheriou and D. Falconer, "Tracking properties and steady-state performance of rls adaptive filter algorithms," *Acoustics, Speech and Signal Processing, IEEE Transactions on*, vol. 34, no. 5, pp. 1097–1110, 1986.
- [47] S. Marcos and O. Macchi, "Tracking capability of the least mean square algorithm: Application to an asynchronous echo canceller," *Acoustics, Speech and Signal Processing, IEEE Transactions on*, vol. 35, no. 11, pp. 1570–1578, 1987.
- [48] M. Hajivandi and W. Gardner, "Measures of tracking performance for the lms algorithm," *Acoustics, Speech and Signal Processing, IEEE Transactions on*, vol. 38, no. 11, pp. 1953–1958, 1990.

- [49] M. Rupp, "Lms tracking behavior under periodically changing systems," in *Proceedings European Signal Processing Conference, Island of Rhodes, Greece*, 1998.
- [50] B. Hassibi, A. Sayed, and T. Kailath, "H optimality of the lms algorithm," *Signal Processing, IEEE Transactions on*, vol. 44, no. 2, pp. 267–280, 1996.
- [51] K. Ozeki, "An adaptive filtering algorithm using an orthogonal projection to an affine subspace and its properties," *IEICE Trans.*, vol. 67, no. 5, pp. 126–132, 1984.
- [52] C. Hansen, *Understanding active noise cancellation*. Taylor & Francis, 2001.